Received: 11 January 2024 | Revised: 16 January 2024 | Accepted: 19 January 2024

DOI: 10.1002/ar.25401

SPECIAL ISSUE ARTICLE

The Anatomical Record WILEY

# Reassessment of the enigmatic "*Prestosuchus*" *loricatus* (Archosauria: Pseudosuchia) from the Middle-Late Triassic of southern Brazil

**Julia B. Desojo**[1,2,3,4] | **Oliver W. M. Rauhut**[4,5]

[1]División Paleontología Vertebrados, Museo de La Plata, Buenos Aires, Argentina

[2]Consejo Nacional de Investigaciones Científicas y Tecnológicas (CONICET), Buenos Aires, Argentina

[3]GeoBioCenter, Ludwig-Maximilians-Universität Munich, Munich, Germany

[4]SNSB – Bayerische Staatssammlung für Paläontologie und Geologie, Munich, Germany

[5]Sektion Paläontologie, Department für Geo- und Umweltwissenschaften, Ludwig-Maximilians-Universität Munich, Munich, Germany

**Correspondence**
Oliver W. M. Rauhut, SNSB – Bayerische Staatssammlung für Paläontologie und Geologie, Richard-Wagner-Str. 10, D-80333 Munich, Germany.
Email: rauhut@snsb.de

**Funding information**
Alexander von Humboldt-Stiftung; Consejo Nacional de Investigaciones Científicas y Técnicas

**Abstract**

Our knowledge of the diversity and evolution of South American Triassic pseudosuchians has greatly improved in the past 15 years, due to new discoveries, but also to the revision of several historically important specimens. One of the earliest descriptions of pseudosuchians from the Triassic of Brazil stems from the classic work of Huene from the first half of the 20th century, who described several species, including such influential taxa as *Rauisuchus tiradentes* or *Prestosuchus chiniquensis*, which have recently been reviewed. The more poorly known proposed second species of *Prestosuchus*, *P. loricatus*, is the focus of the present work. The original material included some elements of the axial skeleton (cervical and caudal vertebrae, ribs, osteoderms) and the hindlimb (ischia, calcaneum, metatarsus), collected from the *Dinodontosaurus* Assemblage Zone of the Chiniquá area, west of São Pedro do Sul. "*Prestosuchus*" *loricatus* shows numerous differences to *P. chiniquensis*, including the shape of cervical neural spines, presence of epipophyses on the cervical vertebrae, presence of a pit in the iliac articulation of the ischium, lack of longitudinal furrows in the dorsolateral surface of the ischial shafts, the more slender calcaneal tuber and a less pronounced ventral pit in the calcaneum, and is thus referred to a new genus, *Schultzsuchus* gen. nov. Phylogenetic analysis indicates an early branching position within Poposauroidea for *Schultzsuchus*, making it the oldest known member of this clade in South America.

**KEYWORDS**

Ladinian-Carnian, Paracrocodylomorpha, Poposauroidea, Rauisuchia, Santa Maria Supersequence, South America

## 1 | INTRODUCTION

In his overview of the fauna of the Santa Maria Supersequence of southern Brazil, van Huene (1938, 1942) described a new taxon of pseudosuchian, *Prestosuchus*, primarily based on a partial, largely articulated skeleton, for which he coined the specific name *Prestosuchus chiniquensis* (see Desojo et al., 2020; Krebs, 1976). This specimen came

from the locality "Weg-Sanga," close to Chiniquá, west of the municipality of São Pedro do Sul (Figure 1). A few other specimens from the area of Chiniquá were referred to the same species, and a fragmentary specimen from the "Cynodontier-Sanga," some 3 km to the north-west of the original locality (Figure 1), was described as a second species of *Prestosuchus*, *P. loricatus*. As the articulated specimen of *P. chiniquensis* (later designated as lectotype of the species by Krebs, 1976) represented one of the most complete "rauisuchid" pseudosuchians known at the time, it became an important reference taxon for these animals. Furthermore, more material was referred to the same

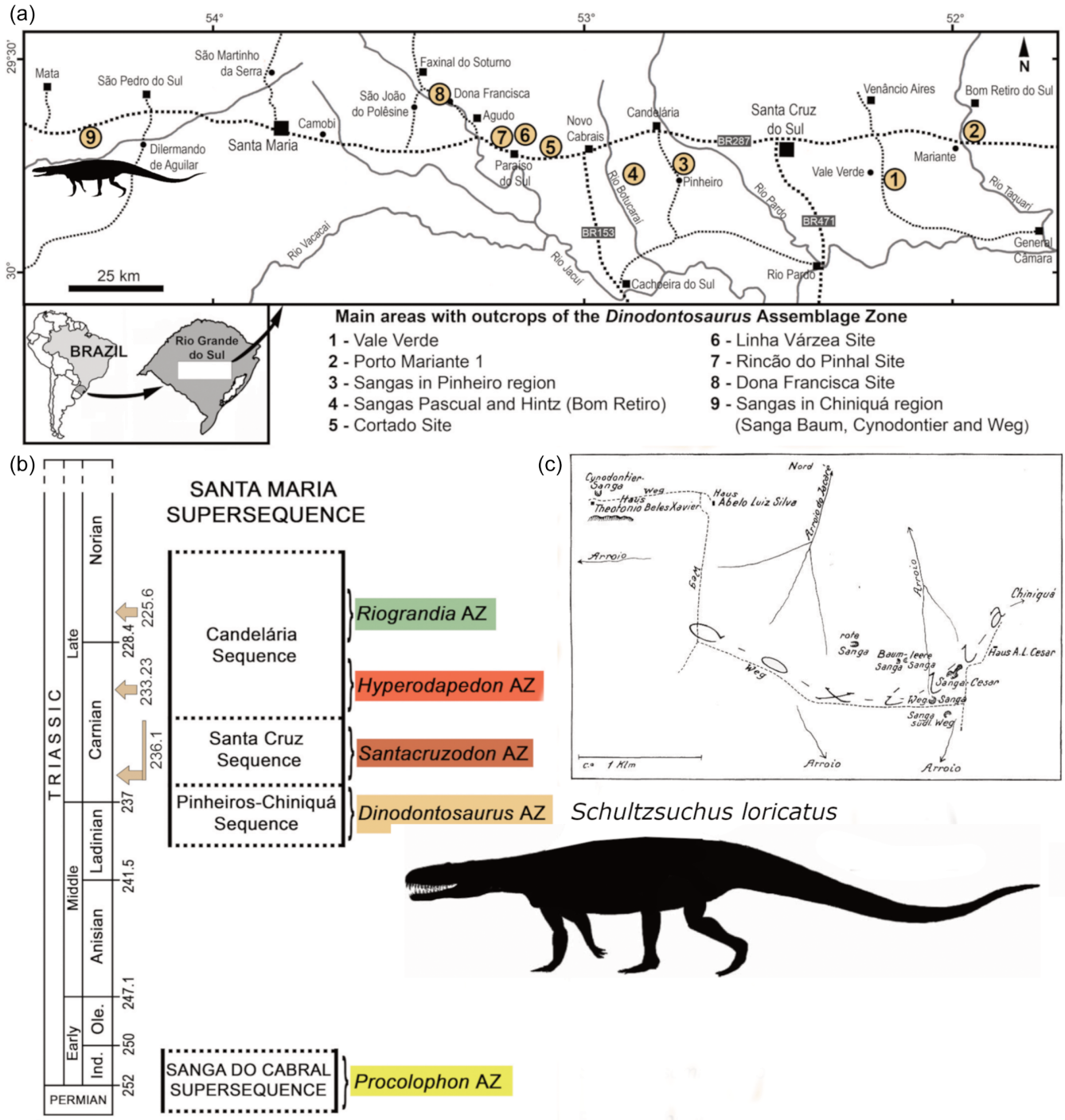


**FIGURE 1** (a) Map of Brazil, showing the location of the *Schultzsuchus loricatus* site (Cynodontier Sanga in Chiniquá region) as indicated by von Huene (1938) within the state of Rio Grande do Sul. Map modified from Schultz et al. (2020). (b) Chronostratigraphic column of the Santa Maria Supersequence, showing the sequence where *Schultzsuchus* was found (*Dinodontosaurus* Assemble Zone). Modified from Schultz et al. (2020). (c), Original Map of the Sangas in the Chiniquá region by von Huene (1942).

taxon over the years, starting with a large, complete skull and partial vertebral column described by Barberena in 1978, and due to the different referred specimens (e.g., Lacerda et al., 2016; Mastrantonio et al., 2013, 2019, 2024; Raugust, 2014; Rezende et al., 2022; Roberto-da-Silva et al., 2018; see also Desojo et al., 2020), *Prestosuchus chiniquensus* is by now one of the best known non-crocodylomorph pseudosuchians. Barberena (1978) and Kuhn (1961, 1976) furthermore independently designated this species as the type species of the genus *Prestosuchus* (but see Kischlat, 2023).

In contrast, the much more poorly known *Prestosuchus loricatus* received little attention in the literature. The specimen is based on a single tooth crown, some vertebral remains, an ischium, calcaneum, a metatarsal, and several osteoderms. A few other elements from the Weg-Sanga (the area of the type locality of *P. chiniquensis*), including a dorsal neural arch, a vertebral centrum, and a calcaneum, were also tentatively referred to *P. loricatus* by von Huene (1942). The latter material was erroneously referred to as "paralectotype of *P. loricatus*" by Desojo et al. (2020), but, as pointed out by Kischlat (2023) and Krebs (1976), this material was only tentatively referred to this species (as indicated by the use of "?" by Huene) and should thus be regarded as referred material. In subsequent publications that commented on *P. loricatus*, this species was considered to be probably synonymous with *P. chiniquensis* by several authors (Barberena, 1978; Krebs, 1976), and this was apparently also accepted by Parrish (1993), who used *Prestosuchus* in his phylogenetic analysis indiscriminantly, and figured materials of the type specimens of both *P. chiniquensis* and *P. loricatus* under this name. However, Krebs (1976, p. 76) also noted that a new analysis of the type specimen of *P. loricatus* would be necessary to establish this synonymy. On the other hand, Kischlat (2002) obviously regarded the type specimen of *P. loricatus* as representing more than a single individual (although this was not clearly stated in this work, but see also Kischlat, 2023, p. 75), as he referred the calcaneum of the type specimen to a newly proposed taxon, *Karamuru vorax* (nomen nudum, see Kischlat, 2023), and described "3 arcos vertebrales" under the name *Abaporu loricatus*, but without previous or further mention of the generic name (see Desojo et al., 2020 and below). Although three vertebral arches are mentioned, their identity is not further clarified, and only one specimen number is given (see below). Kischlat (2002) furthermore provided a short description of characters distinguishing these neural arches from those of *P. chiniquensis*. Desojo et al. (2020) agreed with Kischlat (2002) that the type material of *P. loricatus* represents a different genus than *P. chiniquensis* and suggested further detailed study of these materials. This study is presented here.

### 1.1 | Institutional abbreviations

CPEZ, Coleção Municipal, São Pedro do Sul; Brazil; GPIT, Institut und Museum für Geologie und Paläontologie, Universität Tübingen, Germany; ISI, Geological Studies Unit of the Indian Statistical Institute, Calcutta, India; MACN-Pv, Museo Argentino de Ciencias Naturales "Bernardino Rivadavia", Paleontología de Vertebrados, Buenos Aires, Argentina; MCZD, Museo de Ciencias Naturales y Antropológicas de Mendoza (J. C. Moyano), Mendoza, Argentina; PULR, Paleontología, Universidad Nacional de La Rioja, La Rioja, Argentina; PVL, Paleontología de Vertebrados, Instituto "Miguel Lillo", San Miguel de Tucumán, Argentina; PVSJ, División de Paleontología de Vertebrados del Museo de Ciencias Naturales y Universidad Nacional de San Juan, San Juan, Argentina; QR, National Museum, Bloemfontein, South Africa; SAM, South African Museum, South Africa; SMNS, Staatliches Museum fur Naturkunde, Stuttgart, Germany; SNSB BSPG, Staatliche Naturwissenschaftliche Sammlungen Bayerns, Bayerische Staatssammlung für Paläontologie und Geologie, Munich, Germany; TMM, Texas Memorial Museum, Austin, Texas, USA; TTUP, Texas Tech University Museum, Lubbock, Texas, USA; UCMP, University of California Museum of Paleontology, Berkeley, CA, USA; UFRGS, Universidade Federal do Rio Grande do Sul, Porto Alegre, Brazil; ZPAL, Institute of Paleobiology of the Polish Academy of Sciences in Warsaw, Poland.

## 2 | MATERIALS AND METHODS

The original material of *P. loricatus* was collected by von Huene during his expeditions to the Triassic of Brazil from 1928 to 1929. The material was brought to the University of Tübingen, the workplace of von Huene, where it was prepared and studied. As his expeditions were partially financed by the Bavarian Academy of Sciences, a part of the material, notably a specimen of *Stahleckeria* and the non-dinosaurian archosaur remains, were later transferred to the Bayerische Staatssammlung für Paläontologie (BSPG) in Munich, where they are kept to the present day. Unfortunately, the exact circumstances of the transfer and the original catalogue and specimen numbers were lost when the building of the BSPG was bombed during WW II, and new specimen numbers were given subsequently, as also no numbers were mentioned in the publications of von Huene (1938, 1942). The new main inventory number for the material was AS (=Alte Sammlung, a general acronym for specimens from before the war for which numbers were lost) XXV, with individual specimens being given consecutive

numbers, including the different elements of a single skeleton, such as the lectotype of *Prestosuchus*, which received individual specimen numbers. At some later stage, the main number 1933 L was recovered for the remains from the Huene collection from Brazil in the collections of the BSPG, and the numbers were transferred to this number in the BSPG catalogue. These numbers were referred to by Kischlat (2023). However, the AS XXV numbers are marked on the bones themselves and on the labels kept with the material in the collections, and these numbers have generally been used in the past decades (e.g., Brusatte et al., 2010; Desojo et al., 2020; Ezcurra et al., 2015; Krebs, 1976; Lacerda et al., 2016; Lautenschlager & Rauhut, 2015; Mastrantonio et al., 2019; Nesbitt, 2011; Parrish, 1993; Rezende et al., 2022). To avoid confusion, we thus use these numbers here. It might be worth noting, though, that the consecutive numbers following the main number are the same for both main inventory numbers AS XXV and 1933 L.

The remains of *P. loricatus* came from the "Cynodontier-Sanga," one of the natural trenches in the vicinity of Chiniquá where von Huene collected (Figure 1). According to him (von Huene, 1942, p. 185) they were found c. 30 m away and in a layer 1 m lower than the paralectotype of *P. chiniquensis*. The material was part of his locality 1045, which, apart from the type of *P. loricatus*, has also yielded a partial cervical vertebra referred to *Spondylosoma*, a long bone identified as a partial tibia of a saurischian (see below), and dicynodont and cynodont therapsids (von Huene, 1942, p. 325). Although fragmentary, the material is of matching size and preservation. Furthermore, the serial elements (vertebrae, ribs, osteoderms) show matching morphology, and the fact that the supposed scapula fragment actually represents the iliac peduncle of the ischium and fits onto the preserved ischial shafts also argues for the association of the materials. Thus, we follow von Huene's (1942) assumption that this material most probably belongs to a single individual. It might be worth noting though, that Huene was not completely certain about this, as he mentioned that, "in the case of doubt, the name should be attached to the presacral vertebral remains" (von Huene, 1942, p. 186; see also Kischlat, 2023). The material is currently kept in the collections of the BSPG under the specimen numbers SNSB BSPG AS XXV 13 (cervical neural arch), AS XXV 14 (caudal neural arch), AS XXV 15, 16, 17 (three caudal vertebrae), AS XXV 18, 19 (two partial cervical ribs), AS XXV 20 (tooth), AS XXV 21a, b (two partial dorsal ribs), AS XXV 22 (articulated ischia), AS XXV 23 (distal right metatarsal III), AS XXV 24 (right calcaneum), AS XXV 26a, b (two osteoderms), AS XXV 27 (osteoderm), AS XXV 43 (proximal end of right ischium, described as partial scapula by von Huene, 1942), AS XXV 44 (two articulated osteoderms), AS XXV 45 (partial axial neural arch, described as partial dorsal neural arch by von Huene, 1942), AS XXV 46 (two osteoderms, metatarsal fragment), AS XXV 46a (caudal neural spine), AS XXV 47 (caudal vertebra), and AS XXV 48 (cervical neural arch). von Huene (1942, p. 186) listed a total of six cervical vertebrae fragments, but also described and figured only the three neural arches listed above. Likewise, he listed six caudal vertebrae, but two of these are currently only represented by their neural arch and neural spine, respectively. Again, however, Huene's description and figures of the materials fit the preserved elements. Finally, first von Huene (1942, p. 186) lists only five osteoderms, but later mentions seven such elements in his description (p. 190), a number that fits with the preserved remains.

In order to test the phylogenetic position of *P. loricatus*, we included this taxon in the phylogenetic matrix published by Butler et al. (2022), which incorporated the same character list as Nesbitt, Zawiskie, & Dawley, (2020). We furthermore included the new iliac character proposed by Rezende et al. (2022) and, based on own observations and the literature, we added 14 new postcranial characters and modified four characters of the original list of Nesbitt, Zawiskie, & Dawley, (2020). In addition, we added a further, rather complete specimen of *Prestosuchus*, UFRGS PV 0629 T, recently described by Mastrantonio et al. (2013, 2019, 2024) as an additional operational taxonomic unit (OTU). The primary dataset initially included 103 OTUs, scored for 454 osteological characters (Data S1). Giving the different phylogentic results for the position of *Stagonosuchus nyassicus* in Desojo et al. (2020) and Nesbitt, Zawiskie, and Dawley (2020); also in Butler et al. (2022), we revised all the codings for this taxon, based on direct observations of the original material. Following Nesbitt, Zawiskie, and Dawley (2020), we a priori excluded the following terminal taxa: *Archosaurus rossicus*, *Lewisuchus admixtus*, and *Pseudolagosuchus majori* (combined into *Lewisuchus*, following Ezcurra, Nesbitt, Fiorelli, & Desojo, 2020), *P. loricatus* paralectotype, *P. chiniquensis* lectotype, and *P. chiniquensis* paralectotype, as the latter two were combined in the OTU *Prestosuchus* type series. We furthermore excluded the OTU with all specimens of *Prestosuchus* combined in the *P. chiniquensis* ALL terminal taxon (sensu Nesbitt, Zawiskie, & Dawley, 2020), and preferred analyzing this taxon with different specimens referred to this species as separate OTUs, as in Desojo et al. (2020) and Mastrantonio et al. (2024). Thus, the dataset evaluated the phylogenetic position of "*Prestosuchus*" *loricatus* within a framework of 96 OTUs.

The matrix was analyzed with TNT 1.5 (Goloboff & Catalano, 2016), using a new technology search to find

the shortest tree length 30 times, followed by TBR branch swapping of trees in memory. Both analyses were run using equally weighted parsimony and implied weighing with different *k* values ($k = 3, 6, 9, 12$; Goloboff et al., 2018). The nonarchosauriform archosauromorph *Mesosuchus browni* was set as the outgroup. In case of multiple equally parsimonious trees, we used reduced consensus methods using the IterPCR method (Pol & Escapa, 2009), with the TNT command "pcrprune/>0;nelsen//{0};." Character optimizations and characters supporting different nodes were evaluated using the trace character option of Mesquite (Maddison & Maddison, 2021).

## 3 | SYSTEMATIC PALEONTOLOGY

Archosauria Cope, 1869, sensu Gauthier, 1985.
Pseudosuchia Zittel, 1887–1890 sensu Gauthier, 1985.
Paracrocodylomorpha Parrish, 1993 sensu Nesbitt, 2011.

*Schultzsuchus* nov. gen.

### 3.1 | Type species

*Schultzsuchus loricatus* (von Huene, 1938).

### 3.2 | Etymology

The generic name is in honor of Cesar Schultz, who devoted his career to the discovery and study of the fossil vertebrates from the Santa Maria Supersequence of Brazil.

### 3.3 | Diagnosis

*Schultzsuchus* can be differentiated from all other pseudosuchians by the following characters (autapomorphies are noted with *): axial postzygapophyses more laterally than posteriorly directed and slightly convex anteroposteriorly; axis and postaxial cervicals with epipophyses on the postzygapophyses; articular surface of the mid-cervical prezygapophyses face slightly posterodorsally*; mid-cervical neural pedicles with a sharp edged, medially placed centroprezygapophyseal lamina*; midcervical neural arch without intrapostzygapophyseal lamina*; accessory neural process anterior to the neural spine in middle to posterior caudal vertebrae; presence of a postspinal lamina in the mid-caudal vertebrae, defined by more laterally than posteriorly attaching spinopostzygapophyseal laminae; ridge connecting the pre- and postzygapophyses in the distal caudal vertebrae*; and presence of an ischial pit in the iliac articular surface of the ischium.

### 3.4 | Comment

The species *S. loricatus* was first described as an additional species of the genus *Prestosuchus* by von Huene (1938, 1942). However, the revision of the original material of *Prestosuchus* described by von Huene did not show any clearly shared characters that allow referral to the same genus (Desojo et al., 2020; this work). Apparently, Kischlat (2002) came to the same conclusion, as he listed the species as *Abaporu loricatus* in an overview article of basal archosaurs. However, it is unclear, where the new generic name came from, as no new generic name was formally proposed (in violation of article 16.1 of the ICZN) and the name is not mentioned anywhere else in the text. Furthermore, no type species for the genus *Abaporu* is mentioned, violating article 13.3 of the ICZN. In addition, there is no clear indication of a holotype: although the material of this taxon is cited as "three vertebral arches", only one specimen number is given, as "BSPHG 013." Although we assume that this number refers to SNSB-BSPG AS XXV (=1933 L) 13, this number only includes a single cervical neural arch, and the number "013" is not unique in the numbering system of the BSPG. Therefore, we consider *Abaporu* Kischlat, 2002, to be a nomen nudum and thus propose the new generic name *Schultzsuchus* for *P. loricatus* von Huene, 1938.

### 3.5 | Species

*Schultzsuchus loricatus* (von Huene, 1938).

1938 *P. loricatus* n. sp.; Huene: 147; *partim*
1942 *P loricatus*: n. g. n. sp.; Huene: 161–246
1942 *P. loricatus* (?): Huene: 190–191
1976 *P loricatus*: v. Huene; Krebs: 76
1978 *P. chiniquensis* Huene; Barberena: 64
1981 *P. chiniquensis* Huene; Bonaparte: 82–101; *partim*
1991 *P. chiniquensis* Huene; Azevedo: 19–148; *partim*
1993 *Prestosuchus* Huene; Parrish: 296–297; *partim*
1999 *P. chiniquensis*: Kischlat & Barberena: 53
2000 *Prestosuchus*; Gower: 450–466; *partim*
2002 *Abaporu loricatus* Kischlat: 301

### 3.6 | Holotype

SNSB BSP AS XXV 13–24/26–27/43–48, a tooth fragment and postcranial remains, including a fragment of the axial neural arch, one complete and two partial cervical neural arches, a mid-caudal neural arch, four caudal vertebrae and an isolated caudal neural spine, two partial cervical and two partial dorsal ribs, both articulated ischia, right calcaneum, two metatarsal fragments, and several osteoderms.

### 3.7 | Horizon and age

Cynodontier Sanga (Sanga Theotonio Béles Xavier), west of Chiniquá, Rio Grande do Sul, Brazil. Santa Maria Supersequence, Pinheiros-Chiniquá Sequence, *Dinodontosaurus* Assemblage Zone, probably Middle-Late Triassic (Ladinian-Carnian; Figure 1; see also Schultz et al., 2020).

### 3.8 | Revised diagnosis

As for genus.

### 3.9 | Comments

We restrict the material of *S. loricatus* here to the holotype materials (Krebs, 1976). The referred dorsal vertebrae (SNSB BSPG AS XXV 4, 42) and right calcaneum (SNSB BSPG XXV 25) do not show any shared derived characters with the type of *S. loricatus* and the material was recovered from a different outcrop (Weg Sanga = Sanga da Estrada). Thus, it is removed from the species here. This material was coded in the phylogenetic analysis of Desojo et al. (2020; as "paralectotype of *P. loricatus*") and found to represent an unidentified non-paracrocodylomorph pseudosuchian.

## 4 | DESCRIPTION

### 4.1 | Dentition

The only cranial remain preserved is a tooth fragment (SNSB BSPG AS XXV 20; Figure 2). It consists of the stout tip of a conical tooth. It is notably laterally compressed and recurved and has both mesial and distal serrations, which are, however, largely worn away. As mentioned by von Huene (1942, p. 186), the mesial carina is notably convex apicobasically, whereas the distal carina is straight. The tooth shows 10 mesial denticles per 5 mm,

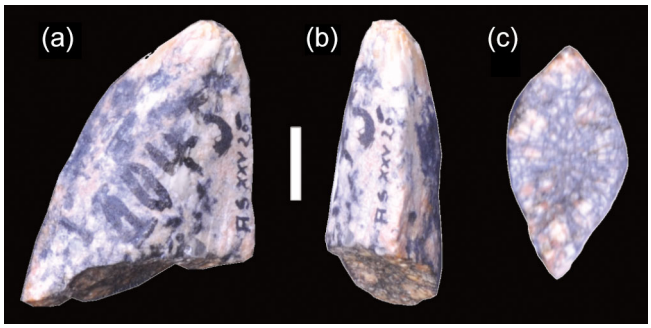


FIGURE 2 *Schultzsuchus loricatus*; tip of a tooth (SNSB BSPG AS XXV 20) in lateral (a), distal (b), and basal (c) view. Scale bar equals 5 mm.

but nothing can be said about the number on the distal carina, due to poor preservation. Unfortunately, the tooth is poorly preserved at the tip and the shape of the denticles is not visible, nor can anything be said about possible enamel structure. The mesial serration extends all the way to the break, where the tooth has a nearly symmetrical, drop-shaped outline (Figure 2c). Internally, the radial arrangement of the dentine is well visible, but there is no trace of the pulpa cavity, indicating that only the very tip of the tooth crown is preserved. Due to the fragmentary nature (not directly associated with any bone) of the element and the reference of von Huene (1938, 1942) that the material was found together with some other vertebrate remains (of synapsids), some uncertainty remains if the tooth belongs to this species. However, the conical recurved tip and the laterally compressed morphology resemble the condition in most Paracrocodylomorpha (e.g., *Saurosuchus galilei* PVSJ 32, *P. chiniquensis* UFRGS-PV-0629-T, *Fasolasuchus tenax* PVL 3050, *Batrachotomus kupferzellensis* SMNS 80269, *Arizonasaurus babbitti* Nesbitt, 2005), ornithosuchids, erpetosuchids, and other carnivorous archosauromorphs, but contrasts with the leaf-like aetosaur teeth, or mesiodistally expanded crowns of *Revueltosaurus callenderi*. The number of 10 serrations per 5 mm resembles the condition in *Heptasuchus clarcki*, with 12 serrations per 5 mm, as described by Nesbitt, Zawiskie, and Dawley (2020).

### 4.2 | Axial skeleton and dermal armor

The axial skeleton of the holotype specimen includes a fragment of the axial neural arch, one almost complete and one fragmentary cervical neural arch (Figure 3), one midcaudal neural arch, and four caudal vertebrae (Figure 4). In addition, two partial cervical and two dorsal ribs are present (Figure 5). For measurements of all skeletal elements see Table 1.

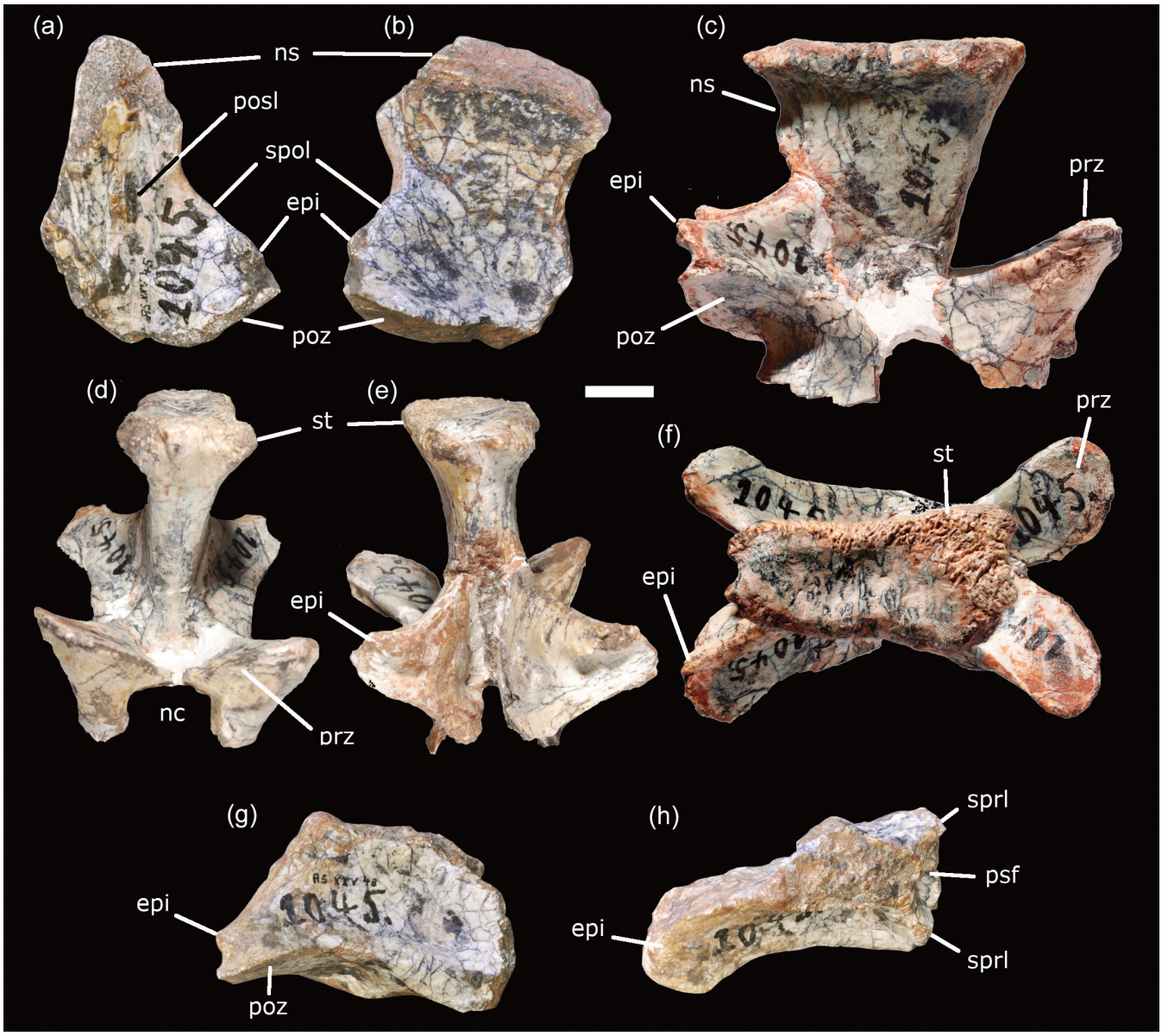


**FIGURE 3** Cervical vertebral remains of the holotype of *Schultzsuchus loricatus*. (a,b) Partial axial neural arch (SNSB-BSPG AS XXV 45) in (a) posterior view; and (b), right lateral view. (c–f) Anterior cervical neural arch (SNSB BSPG AS XXV 13) in (C) right lateral; (d) anterior; (e) posterior; and F, dorsal views. (g,h) Partial posterior cervical neural arch (SNSB BSP AS XXV 48) in (g), right lateral and (h) dorsal views. epi, epiphophysis; nc, neural canal; ns, neural spine; posl, postspinal lamina; poz, postzygapophysis; prz, prezygapophysis; psf, prespinal fossa; spol, spinopostzygapophyseal lamina; sprl, spinoprezygapophyseal lamina; st, spine table. Scale bar equals 1 cm.

### 4.2.1 | Cervical vertebrae

The cervical region is represented by a fragment of the axial neural arch and two incomplete postaxial neural arches.

The axis is represented by the posterior end of the neural spine and the right postzygapophysis (SNSB BSPG AS XXV 45; Figure 3a,b). This element was identified as a dorsal neural arch by von Huene (1942), but the strongly laterally directed postzygapophysis, the posteriorly widening neural spine, and the presence of an epipophysis indicate that it is a cervical element and, more specifically, an axial neural arch. The postzygapophysis is slightly more laterally than posteriorly directed and has a drop-shaped articular surface. The latter has a very slightly anteromedially posterolaterally convex surface and stands at an angle of ~30° from the horizontal. A narrow, ridge-like epipophysis is present on the dorsal surface of the postzygapophysis and connected to the neural spine by a slender, sharp-edged spinopostzygapophyseal lamina (Figure 3a,b). The epipophysis does not overhang the postzygapophysis. In lateral view, the spinopostzygapophyseal lamina is posteriorly concave, as

the neural spine slightly overhangs the posterior end of the neural arch (Figure 3b), as in the axis of *Xilousuchus* (Nesbitt et al., 2011) and *Mandasuchus* (Butler et al., 2017).

The neural spine is incomplete anteriorly and posterodorsally, but a section of the original dorsal margin seems to be preserved (Figure 3b). Thus, the spine extends ~40 mm above the postzygapophysis and has an almost straight, very slightly convex dorsal margin in at least its posterior part. The spine is mediolaterally thin anteriorly, but widens abruptly towards its posterior end, where it is ~16 mm wide dorsal to the spinopostzygapophyseal lamina. The posterior side of the neural spine is inclined anteroventrally and flat, originally obviously forming a wide, but only moderately deep postspinal fossa between the postzygapophyses. In the middle of the posterior surface, a weakly developed midline ridge is present (Figure 3a).

The most complete cervical neural arch SNSB BSPG AS XXV 13 consists of a long and high neural spine that is trapezoidal (dorsally expanding) in lateral view, with both well-developed pre- and postzygapophyses (Figure 3c–f). As preserved, the arch is 67 mm long from the tip of the prezygapophyses to the end of the postzygapophyses, and 56 mm high from the neurocentral suture to the tip of the neural spine.

The zygapophyses project anterolaterally and posterolaterally, respectively, forming an angle of ~90° between the articular surfaces in dorsal or ventral view (Figure 3f). The articular surfaces of the prezygapophyses are longer (c. 20 mm) than wide (c. 16 mm) and have a rounded medial and a straight lateral margin. They are flat, notably inclined posterodorsally, and stand at an angle of ~45° towards each other in anterior view (Figure 3d). The oval articular facets of the postzygapophyses are slightly concave mediolaterally. In anterior view, ventral to the prezygapophysis, the pedicle of the neural arch narrows anteromedially, resulting in a thin lamina that projects from the medial margin of the zygapophysis towards the centrum, thus forming a sharp centroprezygapophyseal lamina (Figure 3d). An equivalent structure is present posteriorly, where a thin lamina extends from the medial margin of the postzygapophysis anteromedioventrally towards the centrum, the centropostzygapophyseal lamina, which also present in some dorsal vertebrae of *Rauisuchus tiradentes* (SNSB-BSPG AS XXV 77, 116, 119). From the lateral side of the postzygapophysis, a robust lamina extends anteroventrally towards the diapophysis, the postzygodiapophyseal lamina (Figure 3c). It becomes less pronounced anteroventrally and levels into the lateral surface towards the mid-length of the neural arch. A prezygodiapophyseal lamina is absent. In dorsal view, the prezygapophyses are separated by a V-shaped incision (Figure 3f), at the posterior end of which a broad, but shallow prespinal fossa is present. This fossa is bordered posterolaterally by short and stout spinoprezygapophyseal laminae, which extend from the posterolateral margin of the prezygapophyseal articular surface posteromedially towards the neural spine. These lamina are very low and extend less than one fifth up the anterior height of the neural spine. Posteriorly, robust spinopostzygapophyseal laminae converge from the postzygapophyses anteromedially towards the neural spine, reaching approximately the half height of the latter structure (Figure 3e). Dorsal to the posterior end of the postzygapophyses, these laminae terminate in robust epipophyses (Figure 3c,e: epi). These are ~9 mm high above the roof of the postzygapophyses and form a medial overhang, so that there is a groove on the posteromedial side of the spinopostzygapophyseal lamina that opens posterolaterally (Figure 3e). The dorsal posterior end of the epipophyses is approximately level with the posterior end of the postzygapophyses or overhangs the latter very slightly. The spinopostzygapophyseal laminae delimit a large, ventrally deeping postspinal fossa. As an interpostzygapophyseal lamina is absent, the fossa has a narrow, elongate, slit-like opening into the neural canal ventrally (Figure 3e).

The neural spine expands from a minimal anteroposterior length of 27 mm just above the dorsal end of the spinopostzygapophyseal lamina to a maximal anteroposterior length of 43 mm at the dorsal end. This expansion is largely gradual, just in the dorsalmost fifth of the spine, the posterior side expands more abruptly. Dorsally, the neural spine is also mediolaterally expanded to form a spine table, which is wider anteriorly than posteriorly, and has striate lateral margins and a slightly mediolaterally concave dorsal surface (Figure 3f). The posterior margin of the spine table is slightly bifurcated. There is a protuberance just above the dorsal ends of the spinopostzygapophyseal lamiae on the posterior margin of the neural spine for the tendon insertion between the neural spines (Figure 3c).

Ventrally, the medial surfaces of the neural pedicels form the margins of the neural canal, which are incompletely preserved, as they seem to have been very thin at the level of the diapophyses. The neural canal was wide (13 mm anteriorly). Most of the pedicles are broken, but a short portion on the right posterior side seems to represent the neurocentral suture. The centrum is not preserved, but it was probably relatively longer than the equivalent cervical centra of the *P. chiniquensis* lectotype (SNSB BSP AS XXV 29, 30) and *Batrachotomus* (Gower & Schoch, 2009).

The posterior cervical neural arch SNSB BSP AS XXV 48 (Figure 3g,h) preserves mainly the right postzygapophysis, with an oval articular facet. In contrast to the neural arch described above, the postzygapophysis seems to have been more posteriorly than posterolaterally directed, and its articular facet seems to have a slight

anteroventral orientation (Figure 3g), in agreement with the posterodorsal orientation of the prezygapophysis in the vertebra described above. A stout spinopostzygapophyseal lamina is also present, connecting the epipophysis with the neural spine (Figure 3g,h). The epipophysis is similar to the one in the more anterior neural arch, but less well developed, and ends slightly anterior to the posterior end of the postzygapophysis. On the anterolateral side of the postzygapophysis, the postzygadiapophyseal lamina is located and extends anteroventrally (Figure 3g). It is less well developed than in the more anterior neural arch and shorter, as the neural arch seems to have been generally shorter than the one described above. Posteriorly, a thin lamina extends from the medial margin of the postzygapophysis anteroventrally towards the centrum. Dorsally the broken base of the neural spine is preserved; it is 25 mm long anteroposteriorly at the break and slightly widens posteriorly (Figure 3h). At the anterior end of the neural spine, the posterior ends of the low, but stout and strongly anteriorly diverging spinoprezygapophyseal laminae are present and delimit the posterior end of a wide prespinal fossa (Figure 3h). The vertebral centrum is not preserved in either of the cervical vertebrae, so it cannot be said if a ventral keel, lateral depressions, and other structures were present or not. The general morphology of the cervical neural spine and laminae resembles that of *Xilousuchus sapingensis* (Nesbitt et al., 2011) and *Arizonasaurus batbbitti* (Nesbitt, 2005), but contrasts with an anteroposterior short spine in *Prestosuchus chiniquensis* (UFRGS-PV-0629-T) and high neural spines in *Rauisuchus tiradentes* (Lautenschlager & Rauhut, 2015), *Batrachotomus kuperferzellensis* (SMNS 80233), *Stagonosuchus nyassicus* (GPIT-PV-3831), *Polonosuchus silesiacus* (ZPAL Ab III 563), and *Postosuchus kirkpatricki* (Weinbaum, 2013). Epiphophysis that do not project more posteriorly than the postzygapophyses are also present in some pseudosuchians, such as the aetosauromorph *Revueltosaurus*, the Poposauroidea *Xilousuchus*, and on the atlantal neural arch of *Effigia* (Nesbitt, 2007, 2011). The elongated prezygapophysis and postzygapophyses resemble those of *Xilousuchus* and *Effigia*, and contrast with the shorter structures in *Rauisuchus tirandentes* (Lautenschlager & Rauhut, 2015), *Prestosuchus chiniquensis* (Mastrantonio et al., 2024), *Batrachotomus kupferzellensis* (SMNS 80233), and *Mambawakale ruhuhu* (Butler et al., 2022).

### 4.2.2 | Caudal vertebrae

There is one caudal neural arch (SNSB BSPG XXV 14) and four isolated caudal vertebrae of different sizes preserved in the holotype, with clear facets for chevrons on the ventral margin of the posterior face of the centrum (SNSB BSPG XXV 15, 16, 17, 47). Furthermore, an isolated posterior midcaudal neural spine is present (SNSB BSPG AS XXV 46a).

SNSB-BSPG XXV 14 is a midcaudal neural arch, preserving the largely complete spine, the postzygapophyses, and a partial left transverse process, while the prezygapophyses are missing (Figure 4a–c). The prezygapophyses were obviously placed on short pedicles and situated entirely lateral to the neural spine. They were connected to the latter by stout, but low spinoprezygapophyseal laminae that delimit a wide, flat prespinal fossa (Figure 4c), similar to the situation in the cervical vertebrae (SNSB-BSPG XXV 13). The transverse process is anteroposteriorly short, placed at about the midlength of the neural arch and laterally and slightly posteriorly directed, but not inclined dorsally (Figure 4a,c). Neither a prezygodiapophyseal lamina nor centrodiapophyseal laminae are present, although the posterior part of the transverse process is slightly thickened. The postzygapophyses are placed slightly higher on the neural arch than the prezygapophyses at the posteroventral base of the neural spine (Figure 4a,b). They are connected to the posterodorsal side of the transverse process by a broad, rounded postzygodiapophyseal lamina and project posteriorly from the base of the neural spine for the entire length of their articular surfaces. The latter flex ventrally medially to form small hypapophyseal laminae that meet just above the neural canal. A stout spinopostzygapophyseal lamina extends from the anterodorsal surface of the postzygapophyses onto the neural spine. In contrast to the situation in the cervical vertebra SNSB-BSPG XXV 13, these laminae attach to the posterior end of the lateral side of the spine, not to its posterior side, and thus leave a thin, but well-developed postspinal lamina in between them (Figure 4a,b). Consequently, a postspinal fossa is small and developed only in between the dorsal surfaces of the postzygapophyses. The neural spine is posteriorly located on the neural arch. It is taller than anteroposterior long and slightly posterodorsally inclined. In contrast to the cervical neural spines, it is mediolaterally thin and lacks a spine table. The dorsal margin of the spine is gently convex anteroposteriorly. The ventral part of the anterior margin is slightly thickened, whereas the dorsal part (above a small broken section) forms a sharp edge.

The caudal vertebral centra are amphicoelus and show a similar general morphology, with oval to almost circular articular facets, and spool-shaped, mediolaterally compressed centra (Figure 4d–j,l,m). Well-developed, separate, triangular chevron facets are present on the posterior margin, whereas the anterior margin is simply markedly flexed ventrally. A marked

**TABLE 1** Measurements (in mm) of selected elements of the lectotype material of "*Prestosuchus*" *loricatus* SNSB BSP AS XXV.

| | |
|---|---|
| Anterior neural spine dorsoventral height (13) | 34.4 |
| Posterior neural spine dorsoventral height (13) | 21.6 |
| Distal neural dorsal spine anteroposterior length (13) | 43.4 |
| Minimal neural spine anteroposterior length (13) | 28.2 |
| Lateromedial neural spine width | 22.4 |
| Cervical prezygapophysis anteroposterior articular surface length | 31.6 |
| Cervical postzygapophysis anteroposterior articular surface length | 23 |
| Cervical prezygapophysis lateromedial articular surface width | 16.2 |
| Cervical postzygapophysis lateromedial articular surface width | 16.4 |
| Right cervical pedicels anteroposterior length | 44.2 |
| Cervical rib length (19) | 34.2* |
| Cervical tuberculum length (19) | 9.4 |
| Cervical rib length (18) | 38.5* |
| Cervical tuberculum length (18) | 5.1 |
| Dorsal rib length (21a) | 124.6 |
| Dorsal tuberculum length (21a) | 13.1 |
| Dorsal rib length (21b) | 94.6* |
| Dorsal tuberculum length (21b) | 12 |
| Anterior caudal centrum length (15) | 39 |
| Medial caudal centrum length (47) | 29 |
| Medial caudal centrum length (16) | 24.2 |
| Posterior caudal centrum length (17) | 19.4 |
| Anterior caudal centrum dorsoventral height (15) | 30.6 |
| Medial caudal centrum dorsoventral height (47) | 18 |
| Medial caudal centrum dorsoventral height (16) | 16.4 |
| Posterior caudal centrum dorsoventral height (17) | 10.3 |
| Medial caudal dorsoventral height (16) | 36.5 |
| Posterior caudal lateromedial width (17) | 16.8 |
| Left ischium dorsal length (22) | 230* |
| Right ischium dorsal length | 218 |
| Height distal left ischium end | 40.8 |
| Height distal right ischium end | 41.2 |
| Right ischium surface for ilium articulation length | 80 |
| Right calcaneum width (24) | 44.6 |
| Right calcaneum length | 60.7 |
| Right calcaneal tuber length | 24.9 |
| Right calcaneal tuber width | 36.6 |
| Right calcaneal tuber height | 41.4 |
| Right calcaneal shaft length | 35.5 |
| Right calcaneal shaft height | 35 |
| Metatarsal length (23) | 44.6* |
| Metatarsal distal width | 20.2 |
| Metatarsal distal height | 15.8 |
| Metatarsal midshaft diameter | 54.8 |
| Osteoderm anteroposterior length (27) | 41.4 |
| Osteoderm anterior width (27) | 23.1 |
| Osteoderm posterior width (27) | 44.8 |
| Osteoderm anteroposterior length (26a) | 33.2 |
| Osteoderm anterior width (26a) | 32.4 |
| Osteoderm posterior width (26a) | 38.7 |
| Osteoderm anteroposterior length (26b) | 31.4 |
| Osteoderm anterior width (26b) | 33.3 |
| Osteoderm posterior width (26b) | 31.6 |
| Osteoderm anteroposterior length (44) | 38.6 |
| Osteoderm anterior width (44) | 23 |
| Osteoderm posterior width (44) | 25 |

*Note*: Asterisk indicates incomplete elements and () specific element number.

ventral groove is present in the most anterior preserved element, a midcaudal (SNSB BSPG AS XXV 15; Figure 4f), and is weakly developed in the more posterior elements, where it is mainly posteriorly defined by low ridges extending from the chevron facets anteriorly (Figure 4h,j,m). The centra are biconcave, with a marked rim around the articular facets, and longer than high, with the relative elongation increasing in more posterior elements (Table 1). Transverse processes are present on the neurocentral suture only in the most anterior caudal vertebra with preserved centrum, SNSB BSPG AS XXV 15 (Figure 4d–f), whereas the vertebrae SNSB BSPG AS XXV AS 47 (Figure 4g), 16 (Figure 4i), and 17 (Figure 4l) show only an anteroposteriorly oriented crest on the suture between the centra and neural pedicels. There is an accessory caudal neural spine (an anterior projection at the base of the neural spine) on the middle to posterior caudal vertebrae SNSB BSPG AS XXV 16 and 47 (Figure 4g,i), resembling that described for *Ticinosuchus ferox* and *Rauisuchus tiradentes* (Lautenschlager & Desojo, 2011). The prezygapophyses are missing in SNSB BSPG AS XV 15 and are incompletely preserved in SNSB BSP AS XXV 16 and 47, projecting anterolaterally with an angle of ~70° between the left and right zygapophysis. The subcircular articular facets are very slightly concave, mainly flat. Stout and strongly anteriorly diverging spinoprezygapophyseal laminae seem to have been present in the most

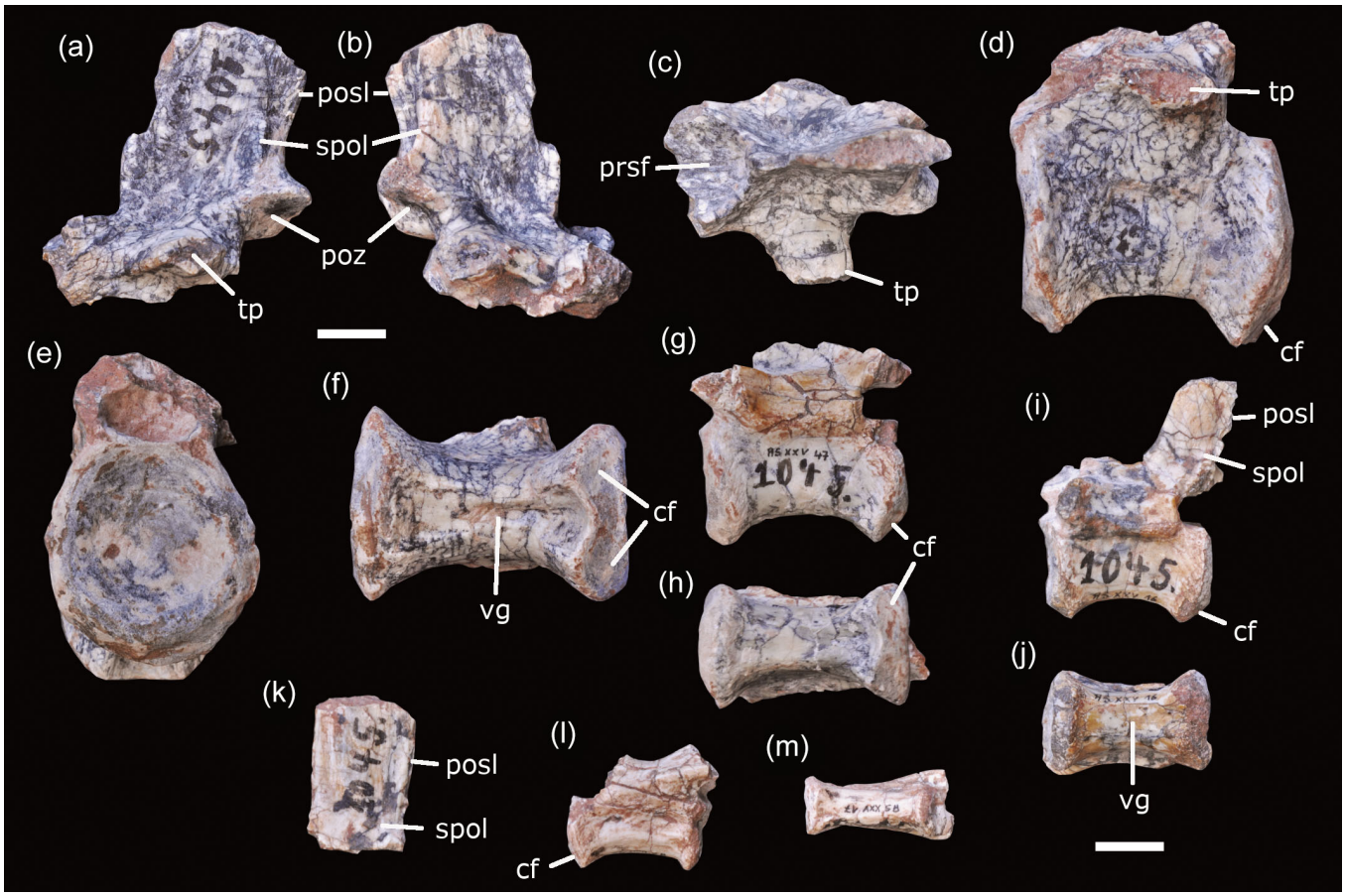


**FIGURE 4** Caudal vertebral remains of the holotype of *Schultzsuchus loricatus*. (a–c), Midcaudal neural arch (SNSB BSPG XXV 14) in (a), left lateral; (b), right lateral; and (c) dorsal views. (d–f), Anterior caudal centrum (SNSB BSPG AS XXV 15) in (d) left lateral; (e) anterior; and (f) ventral views. (g,h) Middle to posterior caudal vertebra (SNSB BSPG AS XXV 47) in (g), left lateral and (h) ventral views. (i,j) Posterior midcaudal vertebra (SNSB BSPG AS XXV 16) in (i) left lateral and (j) ventral views. (k), Isolated caudal neural spine (SNSB BSPG AS XXV 46a) in left lateral view. (l,m) Posterior caudal vertebra (SNSB BSPG AS XXV 17) in (l) right lateral; and (m) ventral views. cf, chevron facet; posl, postspinal lamina; poz, postzygapophysis; prsf, prespinal fossa; spol, spinopostzygapophyseal lamina; tp, transverse process; vg, ventral groove. Scale bar equals 1 cm.

anterior of these vertebrae, similar to the situation in the isolated neural arch SNSB BSPG AS XXV 14, but are absent in more posterior elements. In the most distal caudal vertebra, SNSB BSPG AS XXV 17 (Figure 4l,-m), the neural arch is placed on the anterior three fourths of the centrum and the pedicles of the broken prezygapophyses are massive and project anterodorsally. The postzygapophyses are complete and project slightly posterior to the dorsal centrum margin in SNSB BSPG AS XXV 16 and 47. They are at approximately the same level as the prezygapophyses in the latter, unlike the dorsally displaced zygapophyses in the isolated midcaudal neural arch SNSB BSPG AS XXV 14. A thin lamina between the prezygapophysis and postzygapophysis is present, laterally to the base of the neural spine of SNSB BSPG AS XXV 16 (Figure 4i) and less developed in SNSB BSPG AS XXV 47 (Figure 4g), resembling the condition on *Batrachotomus kupferzellensis* (SMNS 80339), *Polonosuchus silesiacus* (ZPAL Ab III 563), and *Ticinosuchus ferox* (PIMUZ T 2817). The main neural spine is only preserved in the distal caudal SNSB BSPG AS XXV 16 (Figure 4i). It is well separated from the small additional anterior spine, anteroposteriorly short and placed on the posterior end of the neural arch, slightly overhanging the centrum posteriorly in its dorsal part. The spine is mediolaterally thin, rectangular in outline, and slightly posterodorsally inclined. As in the midcaudal neural arch SNSB BSPG AS XXV 14 and the middle to posterior caudal vertebrae of *Rauisuchus* (Lautenschlager & Rauhut, 2015), there seem to be short, laterally placed spinopostzygapophyseal laminae that define a small postspinal lamina (Figure 4i). The isolated neural spine SNSB BSPG AS XXV 46a is somewhat larger than the spine of this vertebra and thus represents a more anterior caudal (Figure 4k). It is also rectangular in outline, very slightly expanding dorsally,

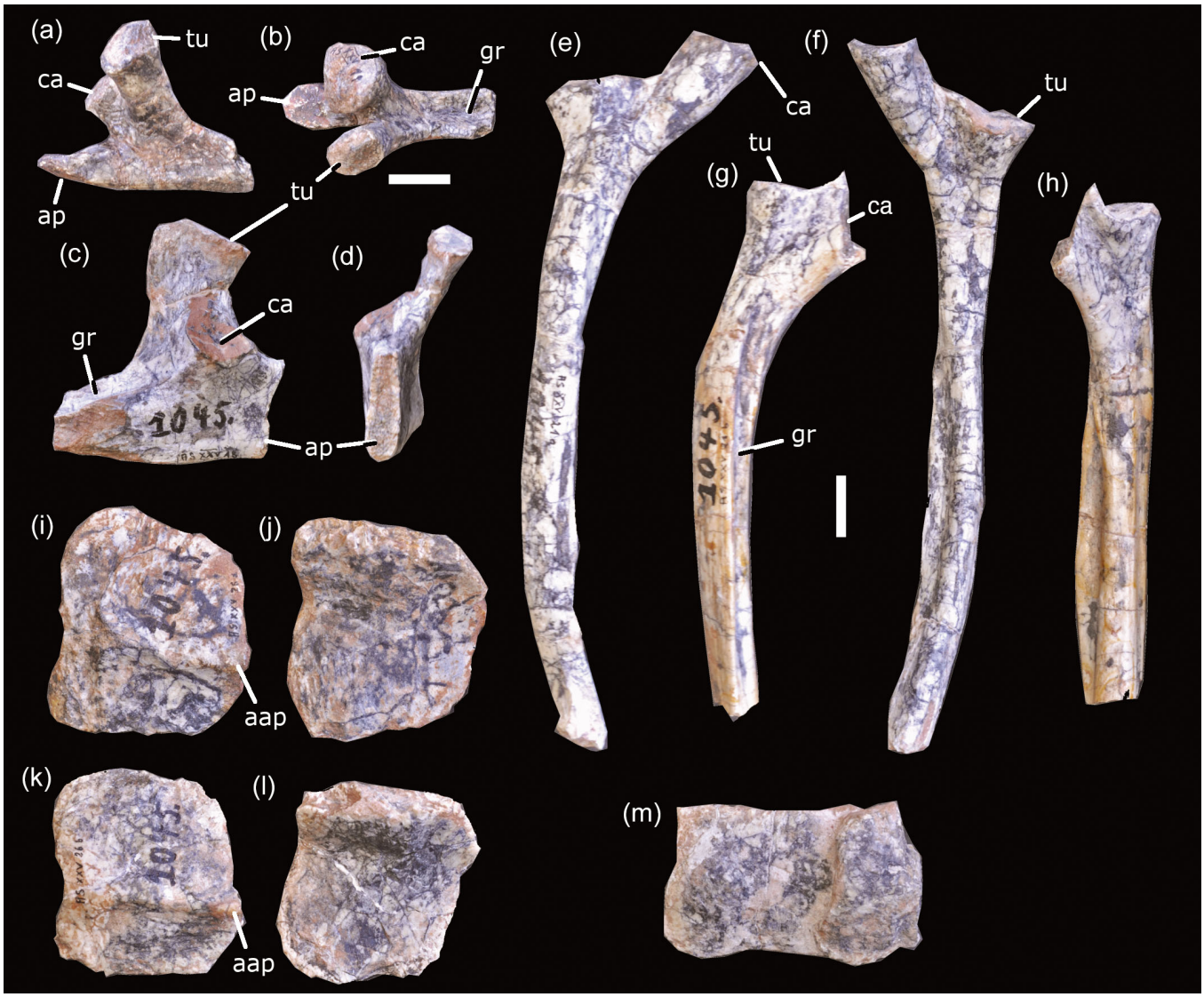


FIGURE 5 Cervical and dorsal ribs and osteoderms of the holotype of *Schultzsuchus loricatus*. (a,b) Anterior cervical rib (SNSB BSPG AS XXV 19) in (a) lateral; and (b) dorsal views. (c,d) Proximal region of posterior cervical rib (SNSB BSPG AS XXV 18) in (c) medial; (d), anterior views. (e–h) Partial right dorsal ribs (SNSB BSP AS XXV21 a,b) in (e,g) anterior and (f,h) medial views. (i,j) Paramedial osteoderm (SNSB BSPG XXV AS 26a) in (i) dorsal, (j) ventral views. (k,l) Paramedial osteoderm (SNSB BSPG XXV AS 26b) in (k) dorsal, (l) ventral views. (m) Articulated osteoderms (SNSB BSPG XXV AS 44) in dorsal view. aap, anterior articular process; ap, anterior process; ca, capitulum; gr, groove; tu, tuberculum. Scale bars equal 1 cm.

and mediolaterally flat. The spinopostzygapophyseal lamina are developed as two notable lateral swellings that delimit the postspinal lamina anteriorly.

The general morphology of the middle and posterior caudals resembles that of *Rauisuchus tiradentes* (Lautenschlager & Rauhut, 2015) and *Ticinosuchus ferox* (PIMUZ T 2817), but contrasts with the anteroposterior shorter centra of *Batrachotomus kupferzellensis* (SMNS 80341) and the robust centra of *Stagonosuchus nyassycus* (Gebauer, 2004), *Prestosuchus chiniquensis* (UFRGS PV 639), *Saurosuchus galilei* (PVSJ 615), and *Fasolasuchus tenax* (PVL 3850).

### 4.2.3 | Ribs

The proximal segments of two cervical ribs (SNSB BSPG XXV 18, 19) are preserved (Figure 5a–d). The ribs are double-headed, with a long and stout tuberculum and a short and slightly larger capitulum, with a circular articular facet of the latter. The turberculum of the SNSB BSP XXV AS 18 is broken. A pronounced dorsomedially facing longitudinal groove is present on the shaft of the rib, behind the confluence of tuberculum and capitulum (Figure 5b,c). The smaller cervical rib SNSB BSPG AS XXV 19 can be referred to an anterior cervical because

the tuberculum and capitulum are not well separated. The ventral and dorsolateral surfaces of the cervical ribs are flat, curving into each other in the dorsoventrally convex lateral surface. In SNSB BSP AS XXV19 a mediolaterally compressed, anteriorly rounded anterior process projects anteriorly a short distance beyond the articular facets (Figure 5a,b). This process, separated by a waisted region from the tuberculum and capitulum, is also present in *Xilosousuchus sapingensis* (Nesbitt et al., 2011), and the poposaurids *Arizonasaurus babbitti* and *Poposaurus langstoni* (Nesbitt, 2005). In SNSB BSPG AS XXV 18, the process is broken off, but its base is strongly compressed dorsolaterally mediventrally and notably high (Figure 5c,d), resembling the keeled middle cervical ribs of *Postosuchus alisonae* (Peyer et al., 2008) and *Batrachotomus kupferzellensis* (SMNS 91046).

The two right dorsal ribs (SNSB BSP AS XXV21 a,b) are double-headed and distally incomplete (Figure 5e–h). SNSB BSPG AS XXV 21b is less complete, but more robust and bears a longitudinal depression in the posterior surface of the shaft; such a depression is only hinted at in the most distal preserved part of the rib shaft in the more slender rib SNSB BSPG AS XXV 21a. The rib shafts are triangular in cross section, with a longitudinal groove in the anteromedial surface, mainly defined by an anteriorly projecting flange on the lateral side of the rib (Figure 5g), as in some ribs of *Batrachotomus kupferzellensis* (SMNS 91044), *Prestosuchus chiniquensis* (SNSB-BSPG AS XXV 9), *Rauisuchus tiradentes* (SNSB-BSPG AS XXV 87c), *Fasolasuchus tenax* (PVL 3850), and *Postosuchus* (Weinbaum, 2013). The anterolateral surface of the shaft is almost flat and the end of SNSB BSPG AS XXV 21a expands distally. Proximally, the tuberculum is considerably shorter than the capitulum and has an elongated oval articular surface in contrast to the round articular surface of the latter (only preserved in SNSB BSPG AS XXV 20a). Proximally, the capitulum and tuberculum are connected by a thin lamina of bone so that there is no clear bifurcation of the proximal rib.

#### 4.2.4 | Osteoderms

There are several paramedian osteoderms preserved (SNSB BSPG XXV AS 26a,b, 27,44,46; Figure 5i–m), some of them articulated with the previous element (SNSB BSPG AS 44). Whereas medially, the medial margins of both osteoderms simply abut each other within one row, the posterior margin of each osteoderm overlaps the anterior margin of the subsequent element, as can be seen in SNSB BSPG AS XXV 44 (Figure 5m). Consequently, the medial side of the osteoderms is slightly thickened, whereas the anterior, lateral, and posterior margins are more sharp-rimmed. The ventral surface of the posterior section of the osteoderms is mediolaterally concave (Figure 5j,l). Two osteoderm morphotypes are present, one asymmetric (i.e., with an anteroposterior dorsal protuberance separating a narrow medial and broad lateral part), and a second type, which is mostly symmetric. The asymmetric osteoderms, including the longer than wide SNSB BSPG AS XXV 44, which has a straight anterior margin and the medial part being slightly smaller than the lateral, and SNSB BSP AS XXV 26a, b, which are wider than long and have a strongly concave basal surface with a small anterior articulation process (Figure 5i–l). The general morphology and histology (Scheyer & Desojo, 2011) of these osteoderms resemble the condition of asymmetrical paired paramedian osteoderms in *Prestosuchus chiniquensis* (SNSB-BSPG AS XXV 7, UFRGS-PV-0156-T, 0629-T, and CPEZ-239b), but contrast with those of *Postosuchus*, which are roughly parallelogram-shaped, with anterior lappets that extend anteriorly from the anterolateral surface (Weinbaum, 2013). The almost symmetric osteoderm SNSB BSP AS XXV 27 is triangular, almost heart shaped, with a centrally placed anterior articular projection and a marked ventral concavity posteriorly on the basal surface. This osteoderm probably belongs to the postsacral region, as in other loricatans (e.g., *Ticinosuchus ferox* PIMUZ 2817, *Fasolasuchus tenax* PVL 3850, *Batrachotomus kupferzellensis* SMNS 90018), but contrasts with the more slender caudal osteoderms of *Rauisuchus tiradentes* (SNSB-BSPG AS XXV 94). The external surface of the osteoderms is ornamented with an anteroposteriorly oriented dorsal keel and smooth ridges radiating laterally from an anteroposterior low central protuberance.

### 4.3 | Appendicular skeleton

The pelvic girdle of the holotype is only known from both articulated ischia (Figure 6), whereas nothing is preserved of the stylopodium and zeugopodium. The right calcaneum is also preserved as the unique proximal tarsal element (Figure 7), as is a fragment of the distal metatarsal 3 of the right pes (Figure 8) and an indeterminate fragment of a metatarsal shaft.

#### 4.3.1 | Ischium

Both ischia are preserved in articulation (SNSB BSPG AS XXV 22; Figure 6a–c), but the proximal end of the right ischium is separated and was originally described as the articular region of the right scapula by von Huene (1942); specimen (SNSB BSPG AS XXV 43). However, the break


**FIGURE 6** Pelvic elements of the holotype of *Schultzsuchus loricatus*. (a–c) Articulated ischia (SNSB BSPG AS XXV 22) in (a) dorsal; (b) right lateral (articulated shafts SNSB BSPG AS XXV 22 and proximal end (SNSB BSPG AS XXV 43); and (c) ventral views. (d,e) Proximal end of the right ischium (SNSB BSPG AS XXV 43) in (d) ventrolateral and (e) dorsal views. ac, acetabulum; ip, ischial pit. Scale bars equal 1 cm.

distal to the articular surface of this bone fits perfectly onto the proximal break of the right ischium (Figure 6b), leaving no doubt that it is part of the same element. The proximal end has a concave articular surface that forms the posteroventral part of the acetabulum and is delimited by a lateroventrally sharp ridge (Figure 6b,d). Dorsally and anteriorly, the acetabular surface flexes medially into the articular facets for the ilium and pubis, respectively. The pubic articulation is incomplete ventrally, but seems to have been narrow and only slightly expanded towards the ventral acetabular rim. The iliac articular surface is narrow anteriorly but expands rapidly laterally posteriorly at the acetabular border (Figure 6e). An oval depression on the iliac articular facet, on the posterior part of the head of the ischium into which the ischial process of the ilium fits, is present and described as the ischial pit in *Poposaurus gracilis* by Weinbaum and Hungerbühler (2007) and is also present in *Bromsgroveia* (Nesbitt, 2005). The articulated ischia are long and stout bones, the suture between them being visible in dorsal and ventral view over the entire length of both elements (Figure 6a,c). Distally, there is a narrow, shallow groove along the interischial suture, but a sharp median ridge arises from this suture on the anterior surface of the articulated ischia directly proximal to the distal end (Figure 6b,c). This ridge gradually becomes more conspicuous and sharp-edged proximally until it rapidly expands into the ischial obturator blade in the proximal third of the bone. Posterodorsally, the interischial suture is marked by a shallow longitudinal groove, which becomes deeper and wider proximally until the proximal ends of

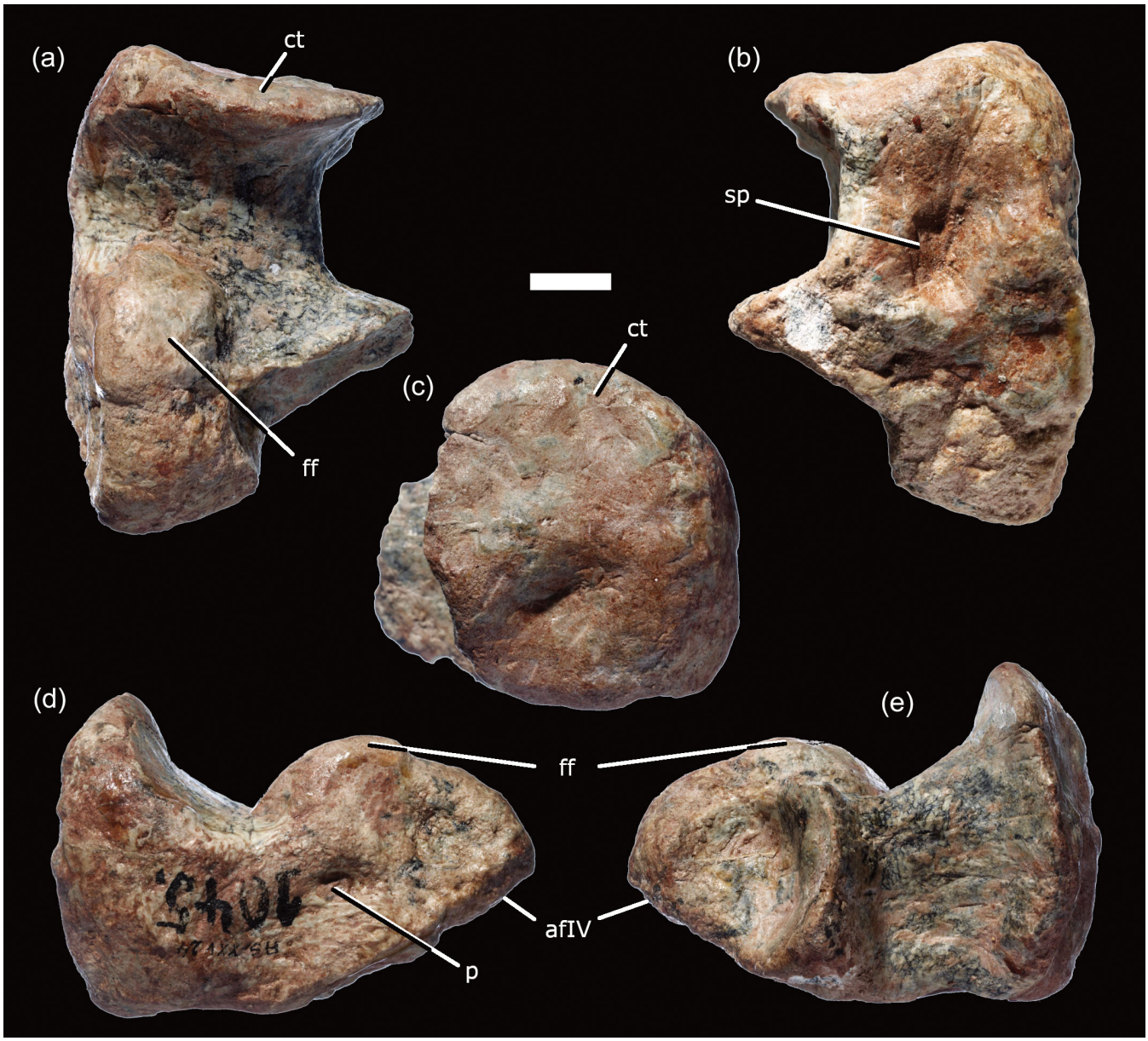


**FIGURE 7** Right calcaneum of the holotype of *Schultzsuchus loricatus* (SNSB BSPG AS XXV 24) in (a) dorsal; (b) ventral; (c) posterior; (d) right lateral; and (e) left lateral views. afIV, articular facet for distal tarsal IV; ct, calcanear tuber; ff, fibular facet; p, pit; sp, shallow pit. Scale bar equals 1 cm.

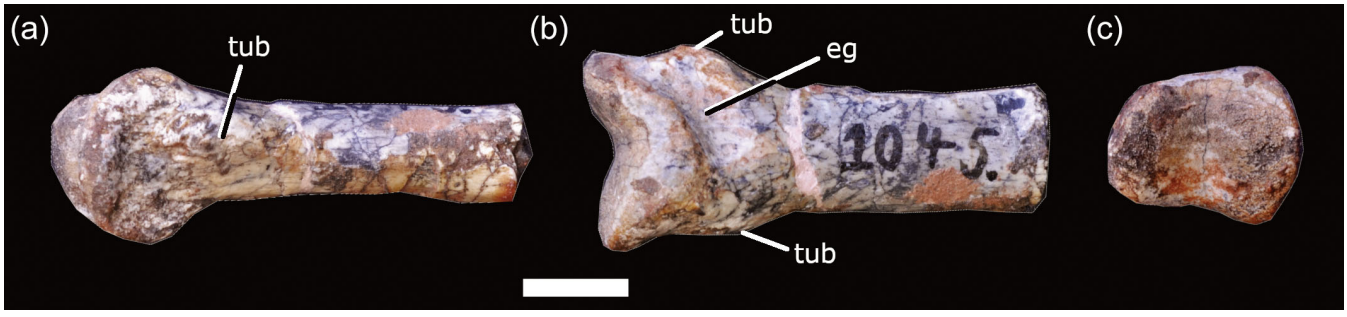


**FIGURE 8** Distal end of the right third metatarsal of the holotype of *Schultzsuchus loricatus* (SNSB BSPG AS XXV 23) in (a) lateral; (b) dorsal; and (c) distal views. eg, extensor groove; tub, tubercle. Scale bar 1 cm.

both ischia separate (Figure 6a). Distal to the groove, the articulated shafts of the ischia are posterodorsally flat, until distally marked dorsolateral edges arise from the lateral margins of the bones and define a wide, shallow median depression on the posterodorsal surface of the distal ischia. No crest and groove are present on the dorsolateral surface of each ischium, in contrast to *Prestosuchus chiniquensis* and *Stagonosuchus nyassicus* (Desojo et al., 2020). The shaft of the ischium is triangular in cross section and becomes more robust distally, resembling the rod-like elements of *Prestosuchus chiniquensis*, *Stagonosuchus nyassycus*, *Saurosuchus galilei*, and *Postosuchus kirckpatricki* (Weinbaum, 2013), contrasting with the thin, flat plate like elements of *Batrachotomus kupferzellensis* and *Poposaurus gracilis* (Weinbaum & Hungerbühler, 2007). The distal end is slightly expanded dorsally and ventrally to form a smooth ischial foot, resembling the condition in *Prestosuchus chiniquensis* (SNSB-BSPG XXV 3), *Stagonosuchus nyassycus* (GPIT/RE/3832), and *Saurosuchus galilei* (PVL 2552), which all have a moderate ischial boot, whereas a different condition, with a thin, ventrally projecting ischiadic boot is present in *Poposaurus*, *Arizonasaurus* and *Batrachotomus* (Nesbitt, 2005, 2011).

### 4.3.2 | Pes

The recovered elements of the right pes consist of the calcaneum and third metatarsal. The ankle articulation is clearly crocodile-normal, with the socket in the calcaneum (Figure 7).

#### *Calcaneum*

The right calcaneum is completely preserved (SNSB BSPG AS XXV 24; Figure 7). The fibular articular facet consists of a hemicylindrical pulley (proximo-anteriorly strongly convex, almost semicircular articular surface), that projects slightly medially anteriorly (Figure 7a,d,e). The distal surface of the calcaneum condyle is flat anteriorly and has an articular facet for distal tarsal IV (Figure 7b,d,e). Medially there is the socket for the peg of the astragalus on the anterior part of the calcaneum that characterizes the crurotarsan archosaurs (Figure 7a,e). The socket is defined posteriorly by a proximodistally concave articular facet that projects medially from the main calcaneum body and has a slightly raised proximal rim (Figure 7e). The lateral surface of the calcaneum body is slightly proximodistally concave anteriorly and flattened posteriorly with a small, shallow pit at the base of the calcaneal tuber (Figure 7d), contrasting with the small, deep pit on the lateral surface of the main body in *Prestosuchus chiniquensis* (Desojo et al., 2020). The posterior region bears the calcaneal tuber, which is anteroposteriorly approximately as long as the main calcaneum body. It expands considerably posteroproximally (Figure 7d,e) and slightly medially (Figure 7a,b). Its posterior end is higher proximodistally than wide mediolaterally (Figure 7c and Table 1), resembling the condition in *Postosuchus alisonae* (Weinbaum, 2013) and *Fasolasuchus tenax* (PVL 3850; Bonaparte, 1981), and contrasting with the rounded outline in posterior view of the calcaneal tuber in *Prestosuchus chiniquensis* (Desojo et al., 2020). Distally, the tuber bears a shallow fossa at its base, and posteriorly it lacks a vertical groove, but is mainly flat proximally, being very slightly convex proximodistally and concave mediolaterally (Figure 7b), contrasting with the large, teardrop-shaped ventral calcanear fossa that deepens posteriorly in *Prestosuchus chiniquensis* (SNSB BSPG AS XXV11c), *Batrachotomus kupferzellensis* (SMNS 90018), and *Postosuchus* (TTUP 9002; Peyer et al., 2008). A shallow depression is present on the distal part of the posterior surface of the tuber.

#### *Metatarsal*

The distal end of the right third metatarsal is almost complete (SNSB BSPG AS XXV 23; Figure 8). In cross section, the shaft is semicircular and dorsoventrally compressed, with a shallow longitudinal groove on the posterior side that disappears towards the distal end. The distal end has a marked oblique depression on the dorsal surface near the articulation facets, representing the extensor groove (Figure 8b), and a shallow lateral depression on the lateral condyle, representing the collateral ligament pit. A corresponding medial depression is only indicated by a slight concavity on the medial side of the distal end (Figure 8a). The distal gynglimus extends approximately as far proximally dorsally as ventrally and is divided into two distinct condyles by a wide, V-shaped incision (Figure 8b,c). The distal articular surface is slightly higher medially than laterally (Figure 8c). Laterally, a rounded tubercle is found at the proximal end of the gynglimus, just proximal to the collateral ligament pit, and a similar, but more dorsally placed tubercle is present also on the medial side (Figure 8a,b). The general morphology resembles those of basal paracrocodylomorphs (*Mambawakale ruhuhu*, Butler et al., 2022; *Prestosuchus chiniquensis*, Desojo et al., 2020), but contrasts with the slender distal metatarsal of *Batrachotomus* (Gower & Schoch, 2009).

## 5 | PHYLOGENETIC POSITION

The equally weighted analysis of the dataset resulted in a total of 78,624 equally parsimonious trees with a length of 1710 steps (CI: 0.312; RI: 0.745). The strict consensus

of these trees shows a relatively good resolution (Figure S1), although with some major polytomies, especially within Pseudosuchia, and concentrated in the early branching members of the clade. Reduced consensus methods identified *Scutellosaurus* as a problematic taxon within Ornithischia on the Avemetatarsalian side of the tree, and *Pagosvenator*, *Xilousuchus*, the supposed *Prestosuchus* specimen CPEZ 239b, *Luperosuchus*, and the supposed *Postosuchus* specimen CM 73372 as problematic within pseudosuchian line archosaurs. A posteriori deletion of these taxa considerably increased resolution of the tree (Figures 9a and S2), with only minor polytomies remaining in the Prestosuchidae (between *Stagonosuchus* and different specimens of *Prestosuchus*), within Rauisuchidae, at the base of Crocodylomorpha, and between some of the higher crocodylomorph taxa.

The analyses using implied weights all resulted in three equally parsimonious trees with scores of 70.76553 ($k = 12$), 86.94684 ($k = 9$), 113.24879 ($k = 6$), and 164.78468 ($k = 3$), respectively. The strict consensus trees of the trees resulting from the analyses with $k = 9$ and $k = 12$ are identical and in agreement with all of the phylogenetic results of the equally weighted analysis (Figures 9b, S3, and S4), but show slightly better

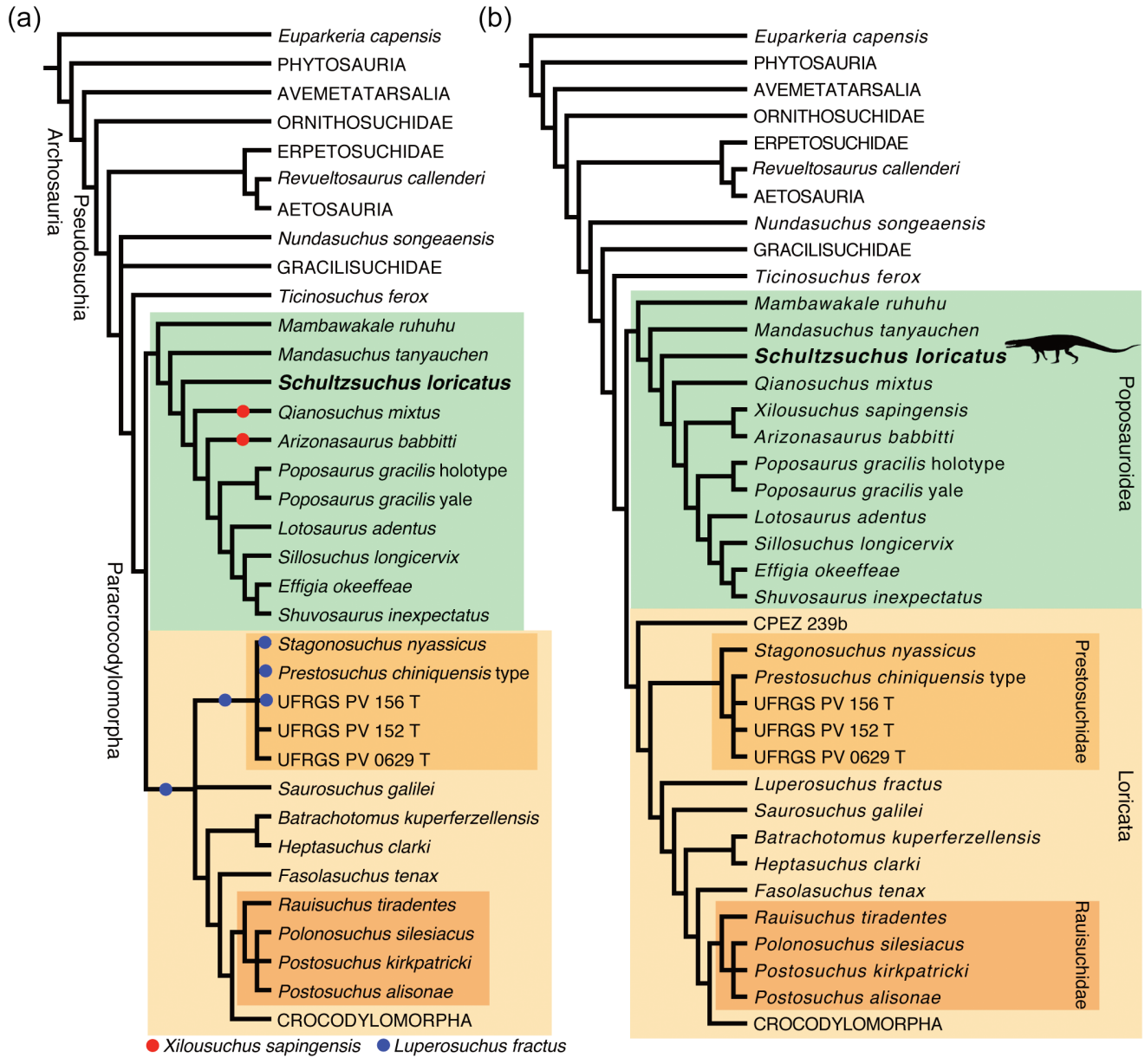


**FIGURE 9** Phylogenetic position of *Schultzsuchus loricatus*. (a) reduced consensus tree of the equally weighted analysis. Possible positions of the problematic taxa *Xilousuchus* and *Luperosuchus* are indicated by colored circles. (b) Strict consensus tree of the analysis using implied weights. Several clades have been collapsed into suprageneric taxa, indicated by upper caps. For complete results see Figures S1–S6.

resolution, and do not require a posteriori deletion of taxa. At higher weighing strengths ($k = 6$ and $k = 3$), *Mandasuchus* and *Schultzsuchus* change positions to be placed within early branching loricatans (Figures S5 and S6). Thus, the former is found in a sister-group relationship with the specimen CPEZ 239b (originally referred to *Prestosuchus*), whereas the latter is placed crownward of *Saurosuchus*. The analysis with the strongest concavity ($k = 3$; Figure S6), furthermore found alternative positions for gracilisuchids, as earliest branching pseudosuchians, and ornithosuchids, which are placed below the erpetosuchid-aetosaur clade. Furthermore, *Nundasuchus* was here recovered as an ornithosuchid. We consider the results with milder concavities ($k = 9$ and $k = 12$), which are more consistent with the unweighted analysis and previous phylogenetic hypotheses, as more reliable. As Goloboff et al. (2018) also found better congruence at higher $k$ values (and specifically at $k = 12$), we mainly use this tree in the further discussion of the results.

Our phylogenetic results are in general agreement with the tree found by Butler et al. (2022) and in earlier iterations of this matrix (e.g., Desojo et al., 2020; Nesbitt, Butler, Ezcurra, Barrett, et al., 2017; Nesbitt & Desojo, 2017; Nesbitt, Zawiskie, & Dawley, 2020). One difference concerns the position of *Nundasuchus*, which was recovered crownwards of Gracilisuchidae by Butler et al. (2022), but as sister taxon to the clade including Gracilisuchidae and Paracrocodylomorpha in our analysis (Figure 9b). This confirms the notion of Butler et al. (2022) that the systematic position of this taxon remains unstable, but its position basal to gracilisuchids also further underlines that *Nundasuchus* most probably is not a paracrocodylomorph. Further differences concern the systematic positions of *Mandasuchus* and *Mambawakale*. These taxa were found in a polytomy at the base of Paracrocodylomorpha by Butler et al. (2022), but are early branching poposaurids in our analysis (Figure 9). However, only one additional step is needed to place *Mambawakale* in Loricata, and three more steps are sufficient for *Mandasuchus* to be placed in this clade. The placement of *Mambawakale* in poposaurids is based on three characters, including the short posterior (subnarial) process of the premaxilla (character 5), the expression of the maxilla in the border of the external nares (character 24), and the concave anterodorsal margin of the base of the ascending process of the maxilla (character 25). Characters uniting *Mandasuchus* with poposaurids include a rounded anterior margin of the antorbital fenestra (character 30, reversal to the ancestral archosaurian condition), the anterior to midcervical centra being longer than the mid-dorsal vertebral centra (character 181, convergently present in many avemetatarsalian archosaurs), and the fan-shaped cervical neural spines (character 439, convergently present in gracilisuchids).

Other differences with the phylogenetic hypothesis of Butler et al. (2022) concern taxa at the base of Loricata that were placed in a monophyletic Prestosuchidae by Desojo et al. (2020), namely *Saurosuchus* and *Stagonosuchus*. The latter was found in a polytomy with poposaurids, *Mandasuchus* and *Mambawakale* by Butler et al. (2022), whereas our analysis confirms a prestosuchid placement for this taxon (Figure 9). *Saurosuchus* was recovered as the earliest branching loricatan by Butler et al. (2022), but is placed crownwards of *Luperosuchus* in the implied weights analysis (Figure 9b; the position of *Luperosuchus* and *Saurosuchus* in respect to prestosuchids and higher loricatans is unresolved in the equal weights analysis; Figure 9a). All other differences only concern better resolution in the implied weights analysis in other parts of the tree, which we will not comment on further here, as they are of no consequence for the focus of this paper.

Concerning the phylogenetic position of *Schultzsuchus loricatus*, the results of all our analyses are congruent in placing this taxon as an early branching poposaurid, as sister taxon to *Qianosuchus* and higher poposaurid taxa (Figure 9). Thus, the phylogenetic analyses further confirm that this taxon is different from *Prestosuchus*. Forcing *Schultzsuchus* into *Prestosuchus* requires at least three additional steps, which, given that only about 11% of characters could be coded for this taxon, makes such a placement rather unlikely. A placement of *Schultzsuchus* in Loricata is at least two steps longer than the shortest trees.

The position of *Schultzsuchus* within poposauroids is based on only two characters, including fan-shaped neural spines in the cervical vertebrae (character 439; unknown in *Mambawakale*, but present in all other poposaurids, including *Mandasuchus*, and convergently present in gracilisuchids and a few nonarchosaurian outgroups), and the presence of epipophyses in the axis (character 441, present in *Schultzsuchus* and *Xilousuchus*, unknown in other poposauroids, and convergently present in aetosaurs and several avemetatarsalian line archosaurs). The placement of *Schultzsuchus* at the base of the Poposauridae is based on several characters present in higher poposauroids, but missing in this taxon, such as the lack of a true spine table in cervical vertebrae (character 191, change from state 2 to state 1), the absence of an anterior spur of the neural spine in middle to distal caudal vertebrae (character 210, the spur is absent in the derived poposaurids *Poposaurus* and *Effigia*, and unknown in most other derived members of the clade),

the absence of a contact between the pubis and ischium (character 287, the contact is absent in all poposaurids more derived than *Qianosuchus*), the presence of a gap between the ventral articular surface for distal tarsal 4 of calcaneum and the distal end of the tuber, but without an associated fossa (character 371, reversal to a nonparacrocodylomorph condition, present in al poposaurids more derived than *Schultzsuchus*), the relatively less broad shaft of the calcaneal tuber (character 376, reversal to the nonparacrocodylomorph condition, present in poposaurids more derived than *Qianosuchus*). Further characters found as autapomorphies of *Schultzsuchus* in the phylogenetic analysis include the presence of pronounced, tubercle-like epipophyses in postaxial cervical vertebrae (character 186, 187, convergently present in *Revueltosaurus*, a few loricatan pseudosuchians and many avemetatarsalian archosaurs), the triangular cross-section of the distal portion of the ischium (character 293, convergently present in some saurischians), the presence of a postspinal lamina that is defined by a laterally directed spinopostzygapophyseal lamina in the caudal vertebrae (character 451, convergently present in loricatans more derived than prestosuchids), and the presence of an ischial pit in the iliac articulation of the ischium (character 452, convergently present in *Poposaurus* and *Shuvosaurus*, but not other poposauroids; see discussion below).

## 6 | DISCUSSION

### 6.1 | Taxonomic distinctiveness and affinities of Schultzsuchus

von Huene (1938, 1942) originally referred *Schultzsuchus loricatus* to the genus *Prestosuchus*, but without giving a detailed justification for the referral to the same genus, mentioning only general similarities of the ischia and calcaneum. As mentioned in the introduction, no further detailed examination of the materials was carried out in more than 50 years, but several authors even considered the two taxa to be probably synonymous (e.g., Barberena, 1978; Krebs, 1976). The first more detailed comment on the materials of *Schultzsuchus loricatus* was presented by Kischlat (2002), who noted the presence of epipophyses in the cervical vertebrae as an important difference from *Prestosuchus chiniquensis* (Kischlat, 2002, p. 301) and argued that this difference warrants generic distinction.

Kischlat (2002) noted that epipophyses are generally absent in pseudosuchians, but present in the dorsal vertebrae of *Sillosuchus* (see Alcober & Parrish, 1997). Nesbitt (2011, p. 109) further discussed the presence of cervical epipophyses in archosaurs, and noted that, within pseudosuchians, these structures are also present in the aetosauromorph *Revueltosaurus*, the poposaurid *Xilousuchus*, on the atlantal neural arch of *Effigia* (see also Nesbitt, 2007), and in the basal loricatan *Batrachotomus*. We further reviewed the distribution of epipophyses and distinguish two morphologies. In some taxa, such as *Xilousuchus* (Nesbitt et al., 2011), or the aphanosaurians *Teleocrater* (Nesbitt, Butler, Ezcurra, Charig, & Barrett, 2017) and *Yarasuchus* (ISI R 334), the epipophyses are developed as small, knob-like protuberances on the dorsal surface of the postzygapophyses, whereas in other taxa, such as *Schultzsuchus*, *Revueltosaurus* (Parker et al., 2022), and many dinosaurs (e.g., Galton, 2014; Sereno & Novas, 1993), the epipophyses are developed as high ridges that are offset from the dorsal surface of the postzygapophysis and often overhang this structure posteriorly. The latter morphology is also present in some further pseudosuchians, including *Stagonosuchus nyassicus* (GPIT PV 60865), *Rauisuchus tiradentes* (Lautenschlager & Rauhut, 2015; SNSB-BSPG AS XXV 75), and *Postosuchus alisonae* (Peyer et al., 2008, figure 3e). On the other hand, we were unable to confirm the presence of epipophyses in the cervical vertebrae of *Batrachotomus* on the basis of direct observations of the material (JBD, pers. obs. 2023; contra Gower & Schoch, 2009; Nesbitt, 2011). Another unusual character in *Schultzsuchus* is the presence of an epipophysis in the axis. Within pseudosuchians, this character is otherwise only present in the aetosauromorphs *Revueltosaurus* (Parker et al., 2022) and *Longosuchus* (TMM 31185), and in the poposaurid *Xilousuchus* (Nesbitt et al., 2011). The character is unknown in other poposauroids, but as *Effigia* has epipophyses on the atlantal neural arch (Nesbitt, 2007), it seems very likely that they were also present in the axis of this taxon. Thus, the presence of axial epipophyses might be a further synapomorphy uniting *Schultzsuchus* with poposaurids.

Another marked difference of *Schultzsuchus* from *P. chiniquensis* (and other basal loricatans) is the shape of the cervical neural spines, as already also commented on by Kischlat (2002). In basal loricatans, including *Prestosuchus*, the cervical spines are usually anteroposteriorly short, high, and elongate rectangular in lateral view, with no or only a slight anteroposterior expansion distally. Furthermore, these spines are thick mediolaterally, so that their anteroposterior length is two times their mediolateral width or less. In contrast, the completely preserved neural arch of *Schultzsuchus* has an anteroposteriorly elongate neural spine with a marked distal expansion, resulting in a fan-shaped outline in lateral view. Within paracrocodylomorphs, this is otherwise found mainly in poposauroids (e.g., *Xilousuchus*, Nesbitt et al., 2011; *Qianosuchus*, Li

et al., 2006; *Arizonasuchus*, Nesbitt, 2005), and in *Mandasuchus*, and is thus another character that indicates poposauroid affinities for *Schultzsuchus* and also for the latter taxon.

Apart from these axial characters, *Schultzsuchus* also differs from *Prestosuchus chiniquensis* in some appendicular features. In the ischium, a deep pit is present in the articular surface for the ilium in *Schultzsuchus*. Such a pit is absent in *Prestosuchus* (Desojo et al., 2020), and is otherwise only found in the poposauroids *Poposaurus* (Schachner et al., 2020; Weinbaum & Hungerbühler, 2007), *Shuvosaurus* (Long & Murry, 1995) and *Bromsgroveia* (Nesbitt, 2005), although it is absent in the poposauroids *Arizonasaurus* (Nesbitt, 2005) and *Sillosuchus* (PVSJ 85). This character could thus be a further synapomorphy of poposauroids (or a subclade thereof), but more research on its distribution is needed. A further difference between the ischia of *Schultzsuchus* and *Prestosuchus* is the lack of a longitudinal depression on the dorsolateral side of the ischial shaft in the former. Such a depression is present in *Prestosuchus* and most other early branching loricatans, but otherwise only known in *Poposaurus* within pseudosuchians (Weinbaum & Hungerbühler, 2007). This character is recovered as a loricatan synapomorphy in our analysis, and its absence in *Schultzsuchus* thus confirms a placement of this taxon outside that clade.

Finally, the calcaneum of *Schultzsuchus* differs from that of *Prestosuchus chiniquensis* in several aspects. In the former taxon, the calcaneal tuber is higher than broad, whereas the opposite is true for *Prestosuchus*, and the ventral pit in the tuber is considerably shallower than in the latter taxon.

As noted in the materials and methods section, the type of *Schultzsuchus loricatus* was found in locality 1045, together with a number of therapsid specimens and two partial bones that were described as saurischian elements by von Huene (1942, pp. 256–258) and identified as a partial cervical vertebral centrum and a tibia, respectively. Given that all the other nontherapsid elements from this locality form the holotype of *S. loricatus*, these two specimens might also belong to the same individual. The vertebra (Galton, 2000, figure 3a–e; von Huene, 1942, figure 51) was considered to represent a saurischian by von Huene (1942) due to the clearly elongate shape of the element, if complete. However, elongate cervical vertebrae are also found in poposauroid pseudosuchians (e.g., Long & Murry, 1995; Nesbitt, 2005, 2007; Nesbitt et al., 2011), and the complete neural arch SNSB BSPG AS XXV 13 of *Schultzsuchus* indicates that this was also the case in this taxon. The vertebra furthermore fits in size with this neural arch and shows a strongly constricted centrum, prominent parapophyses and a ridge-like ventral keel, all characters that are also found in poposauroids (Nesbitt, 2005; Nesbitt et al., 2011). As for the second element, Galton (2000, p. 405) noted that the absence of a cnemial crest argues against an identification as a dinosaurian tibia. This element represents a slender limb bone of fitting size for appendicular elements of especially the forelimb of *Schultzsuchus*, and has some similarities with the ulna of *Effigia* (Nesbitt, 2007), but more detailed comparisons would be necessary to firmly establish its affinities.

## 6.2 | Implications for pseudosuchian diversity, distribution, and phylogeny in the Triassic

The identification of *Schultzsuchus loricatus* as a taxon different from *Prestosuchus* and as a probable early branching poposauroid improves our understanding of Middle Triassic pseudosuchian diversity and distribution in South America. The late Middle Triassic of South America has already yielded a rich diversity of archosauriform taxa, mainly from the Chañares Formation of Argentina (see Ezcurra et al., 2017; Mancuso et al., 2014) and the *Dinodontosaurus* Assemblage Zone of the Santa Maria Supersequence of southern Brazil (Schultz et al., 2020). However, many of the taxa represented are either nonarchosaurian archosauriforms (mainly proterochampsids) or avemetatarsalians, including important findings of early dinosauromorphs and pterosauromorphs from the Chañares Formation (see Ezcurra et al., 2017; Ezcurra, Nesbitt, Bronzati, et al., 2020; Ezcurra, Nesbitt, Fiorelli, & Desojo, 2020). Pseudosuchians are less diverse, and so far represented mainly by erpetosuchids and some of the earliest branching loricatans, plus the gracilisuchid *Gracilisuchus* in the Chañares Formation, and the problematic possible pseudosuchian *Barberenasuchus* (see Irmis et al., 2013) from the *Dinodontosaurus* Assemblage Zone. Thus, paracrocodylomorphan taxa are so far limited to the large predatory loricatans *Luperosuchus* in Argentina and *Prestosuchus* and *Decuriasuchus* (a possible juvenile of *Prestosuchus*; Farias et al., 2023) in Brazil. The identification of *S. loricatus* as a poposauroid thus adds a further lineage of paracrocodylomorphs to this record.

Poposauroids, specifically ctenosauriscids, are among the earliest known pseudosuchians (and, as such, archosaurs in general; see Butler et al., 2011; Ezcurra et al., 2023; Nesbitt et al., 2011). Ctenosauriscids are so far mainly known from the latest Early to early Middle Triassic of the northern Hemisphere (Butler et al., 2011), the exception being the poorly known *Hypselorhachis* from the early Middle Triassic of Tanzania (Butler et al., 2009). As the immediate outgroup of the ctenosauriscid-poposaurid clade, the Chinese taxon

*Qianosuchus*, is also from the northern Hemisphere, a probable Laurasian origin or at least early radiation of poposauroids in this area was indicated. On the other hand, however, all of the earliest branching members of the sister taxon to Poposauroidea, the loricatans, namely *Saurosuchus*, *Luperosuchus*, *Stagonosuchus*, *Prestosuchus*, and *Etjosuchus* (Tolchard et al., 2021) are from the late Middle to early Late Triassic of central to southern Gondwana. With the recognition of the late Middle Triassic *Schultzsuchus* from Brazil and the probably early Middle Triassic Tanzanian pseudosuchians *Mambawakale* (Butler et al., 2022) and *Mandasuchus* as early branching poposauroids, a more Gondwanan origin of Paracrocodylomorpha might be indicated. However, the immediate outgroup of paracrocodylomorphs, *Ticinosuchus*, comes from central Pangea, and, as noted above, the partially older ctenosauriscids seem to have had an almost Pangean distribution already by the early Middle Triassic. Thus, pseudosuchian biogeography in the Pangean world of the Triassic might have been more complex than currently recognized, and more material, especially of early Middle and late Early Triassic pseudosuchians is needed to elucidate their diversification history.

Another aspect of pseudosuchian phylogeny might be noteworthy. Despite the addition of numerous new characters and OTUs to the original phylogenetic analysis of Nesbitt et al. (2011) in the past decade (e.g., Butler et al., 2011, 2014, 2017, 2022; Desojo et al., 2020; Ezcurra et al., 2017; Nesbitt et al., 2014; Nesbitt & Desojo, 2017; Nesbitt, Zawiskie, & Dawley, 2020; Tolchard et al., 2021), the general topology of this hypothesis remains remarkably stable (apart from formerly poorly known clades, such as erpetosuchids, which were only more consistently placed after the recovery or revision and of important taxa and their subsequent addition to the matrix). A notable exception to this general stability might be the early branching members of the Paracrocodylomorpha, in which the phylogenetic position of many of the early branching members of both Poposauroidea and Loricata are still debated. Thus, *Mandasuchus* and *Mambawakale* were found in a polytomy at the base of this clade by Butler et al. (2022), and in our phylogeny, at least an alternative placement of *Mambawakale* at the base of loricatans requires only a single additional step in comparison with the most parsimonious hypothesis. Furthermore, the early branching loricatan taxa *Luperosuchus*, *Saurosuchus*, *Stagonosuchus*, and *Prestosuchus* were found in several different arrangements in recent phylogenies. These range from a monophyletic Prestosuchidae encompassing all of these taxa found by Desojo et al. (2020) to a pectinate arrangement, as found by Butler et al. (2022), and Nesbitt, Zawiskie, and Dawley (2020), in which *Stagonosuchus* was found in a polytomy at the base of Paracrocodylomorpha, with *Saurosuchus* as the earliest branching loricatan, followed by *Prestosuchus* and *Luperosuchus*. Our current hypotheses (implied weighting analyses) again shuffles these taxa around, with *Stagonosuchus* being found as sister taxon to *Prestosuchus* (as in Desojo et al., 2020) and *Saurosuchus* being placed more crownward than *Luperosuchus*. Furthermore, at lower *k* values, also the position of other taxa, such as *Mandasuchus* and *Schultzsuchus* switches from poposauroids to early branching loricatans. Such phylogenetic uncertainty at the base of a major clade might not be too surprising, as many of the early branching taxa are expected to be generally very similar, and homoplasies can be concentrated in basal members (see Rauhut & Pol, 2019). More complete materials and very detailed evaluations of primary homology statements for characters might help to solve this problem.

## AUTHOR CONTRIBUTIONS

**Julia B. B. Desojo:** Conceptualization; methodology; investigation; validation; formal analysis; funding acquisition; writing – original draft; writing—review and editing. **Oliver W. M. Rauhut:** Methodology; data curation; investigation; validation; formal analysis; writing—original draft; writing—review and editing; project administration.

## ACKNOWLEDGMENTS

We thank Georg Janßen for help with the photography and Rainer Schoch (SMNS), Tomasz Sulej (ZPAL), Cesar Schultz (UFRGS), Ingmar Werneburg, and Henrik Stöhr (both GPIT) for help during collection visits. We thank M. Ezcurra, M.B. von Baczko, B. Mastrantonio, S. Nesbitt, and A. Martinelli for critical discussions that helped us to improve the article. Critical reviews by Rodrigo Temp Müller and Flavio Pretto further helped to improve the article, and we thank Leonardo Kerber and Flavio Pretto for editorial assistance. The visits of JBD to Munich were made possible by a fellowship of the Humboldt Foundation and support by the CONICET. The phylogenetic software TNT is provided free of cost by the Willy Hennig Society. Open Access funding enabled and organized by Projekt DEAL.

## ORCID

*Julia B. Desojo* https://orcid.org/0000-0002-2739-3276
*Oliver W. M. Rauhut* https://orcid.org/0000-0003-3958-603X

## REFERENCES

Alcober, O., & Parrish, J. M. (1997). A new poposaurid from the Upper Triassic of Argentina. *Journal of Vertebrate Palaeontology*, *17*(3), 548–556.

Azevedo, S. A. K. (1991). *Prestosuchus chinequensis* Huene 1942 (Reptilia, Archosauria, Thecodontia, Proterosuchia, Rauisuchidae), da Formação Santa Maria, Triássico do Estadodo Rio Grande do Sul, Brasil. Unpublished PhD thesis, Universidade Federal do Rio Grande do Sul, Porto Alegre.

Barberena, M. C. (1978). A huge thecodont skull from the Triassic of Brazil. *Pesquisas, Institute de Geociências, Universidade Federal do Rio Grande do Sul, Porto Alegre*, *9*, 62–75.

Bonaparte, J. F. (1981). Descripción de *Fasolasuchus tenax* y su significado en la sistemática y evolución de los Thecodontia. *Revista del Museo Argentino de Ciencias Naturales "Bernardino Rivadavia"*, *3*, 55–101.

Brusatte, S. L., Benton, M. J., Desojo, J. B., & Langer, M. C. (2010). The higher-level phylogeny of *Archosauria* (Tetrapoda: Diapsida). *Journal of Systematic Palaeontology*, *8*(1), 3–47.

Butler, R. J., Barrett, P. M., Abel, R. L., & Gower, D. J. (2009). A possible ctenosauriscid archosaur from the Middle Triassic Manda Beds of Tanzania. *Journal of Vertebrate Palaeontology*, *29*(4), 1022–1031.

Butler, R. J., Brusatte, S. L., Reich, M., Nesbitt, S. J., Schoch, R. R., & Hornung, J. J. (2011). The sail-backed reptile *Ctenosauriscus* from the latest Early Triassic of Germany and the timing and biogeography of the early archosaur radiation. *PLoS One*, *6*, e25693.

Butler, R. J., Fernandez, V., Nesbitt, S. J., Leite, J. V., & Gower, D. J. (2022). A new pseudosuchian archosaur, *Mambawakale ruhuhu* gen. et sp. nov., from the Middle Triassic Manda Beds of Tanzania. Royal Society Open *Science*, *9*, 211622.

Butler, R. J., Nesbitt, S. J., Charig, A. J., Gower, D. J., & Barrett, P. M. (2017). *Mandasuchus tanyauchen*, gen. et sp. nov., a pseudosuchian archosaur from the Manda Beds (?Middle Triassic) of Tanzania. *Journal of Vertebrate Palaeontology*, *37*(Suppl. 1), 96–121.

Butler, R. J., Sullivan, C., Ezcurra, M. D., Liu, J., Lecuona, A., & Sookias, R. B. (2014). New clade of enigmatic early archosaurs yields insights into early pseudosuchian phylogeny and the biogeography of the archosaur radiation. *BMC Evolutionary Biology*, *14*, 128.

Colbert, E. H. (1987). The Triassic reptile *Prolacerta* in Antarctica. *American Museum Novitates*, *2882*, 1–19.

Cope, E. D. (1869). Synopsis of the extinct Batrachia, Reptilia and Aves of North America. *Transactions of the American Philosophical Society*, *14*, 1–252.

Crush, P. J. (1984). A late Upper Triassic sphenosuchid crocodilian from Wales. *Palaeontology*, *27*(1), 131–157.

Desojo, J. B., von Baczko, M. B., & Rauhut, O. W. M. (2020). Anatomy, taxonomy and phylogenetic relationships of *Prestosuchus chiniquensis* (Archosauria: Pseudosuchia) from the original collection of von Huene, Middle-Late Triassic of southern Brazil. *Palaeontologia Electronica*, *23*, a04.

Ewer, R. F. (1965). The anatomy of the thecodont reptile *Euparkeria capensis* broom. *Philosophical Transactions of the Royal Society B*, *248*, 379–435.

Ezcurra, M. D., Bandyopadhyay, S., Sengupta, D. P., Sen, K., Sennikov, A. G., Sookias, R. B., Nesbitt, S. J., & Butler, R. J. (2023). A new archosauriform species from the Panchet Formation of India and the diversification of Proterosuchidae after the end-Permian mass extinction. *Royal Society Open Science*, *10*, 230387.

Ezcurra, M. D., Desojo, J. B., & Rauhut, O. W. M. (2015). Redescription and phylogenetic relationships of the proterochampsid *Rhadinosuchus gracilis* (Diapsida: Archosauriformes) from the early Late Triassic of southern Brazil. *Ameghiniana*, *52*(4), 391–417.

Ezcurra, M. D., Fiorelli, L. E., Martinelli, A. G., Rocher, S., von Baczko, M. B., Ezpeleta, M., Taborda, J. R. A., Hechenleitner, E. M., Trotteyn, M. J., & Desojo, J. B. (2017). Deep faunistic turnovers preceded the rise of dinosaurs in southwestern Pangaea. *Nature Ecology & Evolution*, *1*, 1477–1483.

Ezcurra, M. D., Nesbitt, S. J., Bronzati, M., Dalla Vecchia, F. M., Agnolin, F. L., Benson, R. B. J., Egli, F. B., Cabreira, S. F., Evers, S. W., Gentil, A. R., Irmis, R. B., Martinelli, A. G., Novas, F. E., da Silva, L. R., Smith, N. D., Stocker, M. R., Turner, A. H., & Langer, M. C. (2020). Enigmatic dinosaur precursors bridge the gap to the origin of Pterosauria. *Nature*, *588*, 445–449.

Ezcurra, M. D., Nesbitt, S. J., Fiorelli, L. E., & Desojo, J. B. (2020). New specimen sheds light on the anatomy and taxonomy of the early Late Triassic dinosauriforms from the Chañares Formation, NW Argentina. *Anatomical Record*, *303*, 1398–1438.

Farias, B. D. M., Desojo, J. B., Cerda, I. A., Ribeiro, A. M., Ferigolo, J., Carlisbino, T., Schultz, C. L., Mastrantonio, B. M., & Soares, M. B. (2023). Bone histology supports gregarious behavior and an early ontogenetic stage to *Decuriasuchus quartacolonia* (Pseudosuchia: Loricata) from the Middle-Late Triassic of Brazil. *Anatomical Record*, 1–17. https://doi.org/10.1002/ar.25365

Galton, P. M. (2000). Are *Spondylosoma* and *Staurikosaurus* (Santa Maria Formation, Middle-Upper Triassic, Brazil) the oldest saurischian dinosaurs? *Paläontologische Zeitschrift*, *74*(3), 393–423.

Galton, P. M. (2014). Notes on the postcranial anatomy of the heterodontosaurid dinosaur *Heterodontosaurus tucki*, a basal ornithischian from the Lower Jurassic of South Africa. *Revue de Palebiologie*, *33*(1), 97–141.

Gebauer, E. V. I. (2004). Neubeschreibung von *Stagonosuchus nyassicus* v. Huene, 1938 (Thecodontia, Rauisuchia) aus der Manda-Formation (Mittlere Trias) von Südwest-Tansania. *Neues Jahrbuch für Geologie Und Paläontologie, Abhandlungen*, *231*(1), 1–35.

Goloboff, P. A., & Catalano, S. A. (2016). TNT version 1.5, including a full implementation of phylogenetic morphometrics. *Cladistics*, *32*, 221–238.

Goloboff, P. A., Torres, A., & Arias, J. S. (2018). Weighted parsimony outperforms other methods of phylogenetic inference under models appropriate for morphology. *Cladistics*, *34*, 407–437.

Gow, C. E. (1975). The morphology and relationships of *Youngina capensis* Broom and *Prolacerta broomi* Parrington. *Palaeontologia africana*, *18*, 89–131.

Gower, D. J. (2000). Rauisuchian archosaurs (Reptilia, Diapsida): An overview. *Neues Jahrbuch für Geologie Und Paläontologie, Abhandlungen*, *218*(3), 447–488.

Gower, D. J. (2001). Possible postcranial pneumaticity in the last common ancestor of birds and crocodilians: Evidence from *Erythrosuchus* and other Mesozoic archosaurs. *Naturwissenschaften*, *88*, 119–122.

Gower, D. J., & Schoch, R. (2009). Postcranial anatomy of the rauisuchian archosaur *Batrachotomus kupferzellensis*. *Journal of Vertebrate Paleontology*, *29*(1), 103–122.

Irmis, R. B., Nesbitt, S. J., & Sues, H.-D. (2013). Early Crocodylomorpha. *Geological Society London, Special Publications*, *379*, 275–302.

Kischlat, E.-E. (2002). Tecodôncios: A Aurora dos Arcossáurios no Triássico. In M. Holz & L. F. De Ros (Eds.), *Paleontologia do Rio Grande do Sul* (pp. 246–272). Universidade Federal do Rio Grande do Sul.

Kischlat, E.-E. (2023). A new nominal genus for "*Prestosuchus*" *chiniquensis* Huene, 1938 (Triassic of southern Brazil): *Huenesuchus* genus novus et combinatio nova. *Revista Brasileira de Paleontologia*, *26*(2), 69–96.

Kischlat, E.-E., & Barbarena, M. C. (1999). *Prestosuchus chiniquensis* (Crurotarsi, Archosauria) does not need a neotype! *Paleontologia Em Destaque, Boletim Informativo da Sociedade Brasileira de Paleontologia*, *14*(26), 53.

Krebs, B. (1976). Pseudosuchia. In O. Kuhn (Ed.), *Handbuch der Paläoherpetologie. Teil 13: Thecodontia* (pp. 40–98). Gustav-Fischer-Verlag, München.

Kuhn, O. (1961). Pars 99. Reptilia (Supplementum 1(2)). In F. Westphal (Ed.), *Fossilium Catalogus. I: Animalia* (pp. 1–163). Uitgeverij Dr. W. Junk, the Hague.

Lacerda, M. B., Mastrantonio, B. M., Fortier, D. C., & Schultz, C. L. (2016). New insights on *Prestosuchus chiniquensis* Huene, 1942 (Pseudosuchia, Loricata) based on new specimens from the "tree Sanga" outcrop, Chiniquá region, Rio Grande do Sul, Brazil. *PeerJ*, *4*, e1622.

Lautenschlager, S., & Desojo, J. B. (2011). Reassessment of the Middle Triassic rauisuchian archosaurs *Ticinosuchus ferox* and *Stagonosuchus nyassicus*. *Paläontologische Zeitschrift*, *85*(4), 357–381.

Lautenschlager, S., & Rauhut, O. W. M. (2015). Osteology of *Rauisuchus tiradentes* from the Late Triassic (Carnian) Santa Maria Formation of Brazil, and its implications for rauisuchid anatomy and phylogeny. *Zoological Journal of the Linnean Society*, *173*, 55–91.

Li, C., Wu, X.-C., Cheng, Y.-N., Sato, T., & Wang, L. (2006). An unusal archosaurian from the marine Triassic of China. *Naturwissenschaften*, *93*, 200–206.

Long, R. A., & Murry, P. A. (1995). Late Triassic (Carnian and Norian) tetrapods from the southwestern United States. *New Mexico Museum of Natural History & Science Bulletin*, *4*, 1–254.

Maddison, W. P., & Maddison, D. R. (2021). Mesquite: A modular system for evolutionary analysis. Version 3.7. http://mesquiteproject.org

Mancuso, A. C., Gaetano, L. C., Leardi, J. M., Abdala, F., & Arcucci, A. B. (2014). The Chañares Formation: A window to a Middle Triassic tetrapod community. *Lethaia*, *47*, 244–265.

Mastrantonio, B. M., Lacerda, M. B., Farias, B. D. M., Pretto, F. A., Rezende, L. D. O., Desojo, J. B., & Schultz, C. L. (2024). Postcranial anatomy of *Prestosuchus chiniquensis* (Archosauria: Loricata) from the Triassic of Brazil. *Anatomical Record*, 1–32. https://doi.org/10.1002/ar.25383

Mastrantonio, B. M., Schultz, C. L., Desojo, J. B., & Garcia, J. B. (2013). The braincase of *Prestosuchus chiniquensis* (Archosauria: Suchia). *Geological Society, London, Special Publications*, *379*, 425–440.

Mastrantonio, B. M., von Baczko, M. B., Desojo, J. B., & Schultz, C. L. (2019). The skull anatomy and cranial endocast of the pseudosuchid archosaur *Prestosuchus chiniquensis* from the Triassic of Brazil. *Acta Palaeontologica Polonica*, *64*, 171–198.

Nesbitt, S. J. (2005). Osteology of the Middle Triassic pseudosuchian archosaur *Arizonasaurus babbitti*. *Historical Biology*, *17*, 19–47.

Nesbitt, S. J. (2007). The anatomy of *Effigia okeeffeae* (Archosauria, Suchia), theropod-like convergence, and the distribution of related taxa. *Bulletin of the American Museum of Natural History*, *302*, 1–84.

Nesbitt, S. J. (2011). The early evolution of archosaurs: Relationships and the origin of major clades. *Bulletin of the American Museum of Natural History*, *352*, 1–292.

Nesbitt, S. J., Butler, R. J., Ezcurra, M. D., Barrett, P. M., Stocker, M. R., Angielczyk, K. D., Smith, R. M. H., Sidor, C. A., Niedzwiedzki, G., Sennikov, A. G., & Charig, A. J. (2017). The earliest bird-line archosaurs and the assembly of the dinosaur body plan. *Nature*, *544*, 484–487.

Nesbitt, S. J., Butler, R. J., Ezcurra, M. D., Charig, A. J., & Barrett, P. M. (2017). The anatomy of *Teleocrater rhadinus*, an early avemetatarsalian from the lower portion of the Lifua Member of the Manda Beds (Middle Triassic). *Journal of Vertebrate Palaeontology*, *37*(Suppl. 1), 142–177.

Nesbitt, S. J., & Desojo, J. B. (2017). The osteology and phylogenetic position of *Luperosuchus fractus* (Archosauria: Loricata) from the latest Middle Triassic or earliest Late Triassic of Argentina. *Ameghiniana*, *54*, 261–282.

Nesbitt, S. J., Langer, M. C., & Ezcurra, M. D. (2020). The anatomy of *Asilisaurus kongwe*, a Dinosauriform from the Lifua Member of the Manda Beds (~Middle Triassic) of Africa. *The Anatomical Record*, *303*(4), 813–873.

Nesbitt, S. J., Liu, J., & Li, C. (2011). A sail-backed suchian from the Heshanggou Formation (Early Triassic: Olenekian) of China. *Earth and Environmental Science Transactions of the Royal Society of Edinburgh*, *101*, 271–284.

Nesbitt, S. J., Sidor, C. A., Angliecyk, K. D., Smith, R. M. H., & Tsuji, L. A. (2014). A new archosaur from the Manda Beds (Anisian, Middle Triassic) of southern Tanzania and its implications for character state optimizations at Archosauria and Pseudosuchia. *Journal of Vertebrate Paleontology*, *34*(6), 1357–1382.

Nesbitt, S. J., Zawiskie, J. M., & Dawley, R. M. (2020). The osteology and phylogenetic position of the loricatan (Archosauria: Pseudosuchia) *Heptasuchus clarki*, from the ? Mid-Upper Triassic, southeastern big Horn Mountains, Central Wyoming (USA). *PeerJ*, *8*, e10101.

Parker, W. G., Nesbitt, S. J., Irmis, R. B., Martz, J. W., Marsh, A. D., Brown, M. A., Stocker, M. R., & Werning, S. (2022). Osteology and relationships of *Revueltosaurus callenderi* (Archosauria: Suchia) from the Upper Triassic (Norian) Chinle Formation of Petrified Forest National Park, Arizona, United States. *Anatomical Record*, *305*, 2353–2414.

Parrish, J. M. (1993). Phylogeny of the Crocodylotarsi, with reference to archosaurian and crurotarsian monophyly. *Journal of Vertebrate Paleontology*, *13*(3), 287–308.

Peyer, K., Carter, J. G., Sues, H.-D., Novak, S. E., & Olsen, P. E. (2008). A new suchian archosaur from the Upper Triassic of North Carolina. *Journal of Vertebrate Palaeontology*, *28*(2), 363–381.

Pol, D., & Escapa, I. (2009). Unstable taxa in cladistic analysis: Identification and the assessment of relevant characters. *Cladistics*, *25*(5), 515–527.

Raugust, T. (2014). Descrição e análise filogenética de um novo material de Rauisuchia (Archosauria, Crurotarsi) da Formação

Santa Maria, Triássico Médio Sul-RioGrandense, Brasil. Unpublished PhD Thesis, Universidade Federal do Rio Grande do Sul, Porto Alegre.

Rauhut, O. W. M., & Pol, D. (2019). Probable basal allosauroid from the early Middle Jurassic Cañadón Asfalto Formation of Argentina highlights phylogenetic uncertainty in tetanuran theropod dinosaurs. *Scientific Reports*, *9*, 18826.

Rezende, L. D. O., Da Rosa, Á. A. S., Lacerda, M. B., & Pretto, F. A. (2022). New Loricata remains from the Pinheiros-Chiniquá sequence (Middle-Upper Triassic), southern Brazil. *Journal of South American Earth Sciences*, *120*, 104089.

Roberto-da-Silva, L., Müller, R. T., de França, M. A. G., Cabreira, S. F., & Dias-da-Silva, S. (2018). An impressive skeleton of the giant top predator *Prestosuchus chiniquensis* (Pseudosuchia: Loricata) from the Triassic of southern Brazil, with phylogenetic remarks. *Historical Biology*, *32*, 976–995.

Schachner, E. R., Irmis, R. B., Huttenlocker, A. K., Sanders, R. K., Cieri, R. L., & Nesbitt, S. J. (2020). Osteology of the Late Triassic bipedal archosaur *Poposaurus gracilis* (Archosauria: Pseudosuchia) from Western North America. *Anatomical Record*, *303*, 874–917.

Scheyer, T. M., & Desojo, J. B. (2011). Palaeohistology and external microanatomy of *Rauisuchian osteoderms* (Archosauria: Pseudosuchia). *Palaeontology*, *54*(6), 1289–1302.

Schultz, C. L., Martinelli, A. G., Soares, M. B., Pinheiro, F. L., Kerber, L., Horn, B. L. D., Pretto, F. A., Müller, R. T., & Melo, T. P. (2020). Triassic faunal successions of the Paraná Basin, southern Brazil. *Journal of South American Earth Sciences*, *104*, 102846.

Sereno, P. C., & Novas, F. E. (1993). The skull and neck of the basal theropod *Herrerasaurus ischigualastensis*. *Journal of Vertebrate Paleontology*, *13*(4), 451–476.

Sulej, T. (2005). A new rauisuchian reptile (Diapsida: Archosauria) from the Late Triassic of Poland. *Journal of Vertebrate Paleontology*, *25*(1), 78–86.

Tolchard, F., Smith, R. M. H., Arcucci, A. B., Mocke, H., & Choiniere, J. N. (2021). A new 'rauisuchian' archosaur from the Middle Triassic Omingonde Formation (Karoo Supergroup) of Namibia. *Journal of Systematic Palaeontology*, *19*(8), 593–631.

von Baczko, M. B., Desojo, J. B., & Ponce, D. (2020). Postcranial anatomy and osteoderm histology of *Riojasuchus tenuisceps* and a phylogenetic update on Ornithosuchidae (Archosauria, Pseudosuchia). *Journal of Vertebrate Paleontology*, *39*(5), e1693396.

von Huene, F. (1938). Die fossilen Reptilien des südamerikanischen Gondwanalandes. Ergebnisse der Sauriergrabungen in Südbrasilien 1928/29. *Neues Jahrbuch für Mineralogie, Geologie Und Paläontologie*, *1938*(3), 142–151.

von Huene, F. (1942). *Die fossilen Reptilien des südamerikanischen Gondwanalandes*. C.H. Beck'sche Verlagsbuchhandlung.

Weinbaum, J. C. (2013). Postcranial skeleton of *Postosuchus kirkpatricki* (Archosauria: Paracrocodylomorpha), from the Upper Triassic of the United States. *Geological Society London, Special Publications*, *379*, 525–553.

Weinbaum, J. C., & Hungerbühler, A. (2007). A revision of *Poposaurus gracilis* (Archosauria: Suchia) based on two new specimens from the Late Triassic of the southwestern USA. *Paläontologische Zeitschrift*, *81*(2), 131–145.

Zittel, K. A. (1887–1890). *Handbuch der Palaeontologie. Abteilung Palaeozoologie*. R. Oldenbourg, München & Leipzig.

## SUPPORTING INFORMATION

Additional supporting information can be found online in the Supporting Information section at the end of this article.

**How to cite this article:** Desojo, J. B., & Rauhut, O. W. M. (2024). Reassessment of the enigmatic "*Prestosuchus*" *loricatus* (Archosauria: Pseudosuchia) from the Middle-Late Triassic of southern Brazil. *The Anatomical Record*, 1–27. https://doi.org/10.1002/ar.25401

## APPENDIX A: CHARACTER CHANGES TO BUTLER ET AL.

### A.1. EMENDED CHARACTERS

**Character 186**. Epipophyses: (0) absent in postaxial cervical vertebrae; (1) present, developed as a small tuberance dorsal to the postzygapophysis; (2) present, developed as a stout tubercle that projects considerably dorsally from the roof of the postzygapophysis (ordered).

Nesbitt et al. (2011) originally only coded for the absence/presence of epipophyses in anterior cervicals. However, there is a notable difference in the development of these processes in different archosaurs. In *Xilousuchus* (Nesbitt et al., 2011) and *Teleocrater* (Nesbitt, Butler, Ezcurra, Charig, & Barrett, 2017), the epipophysis are very small dorsal protuberances on the dorsal surface of the postzygapophyses. In contrast, in many other archosaurs were these processes are present, such as *Rauisuchus* (SNSB BSPG AS XXV), *Stagonosuchus* (GPIT RE 3831), *Schultzsuchus loricatus*, and dinosaurs, they are high, notably projecting dorsally from the postzygapophyses. Thus, we added an additional state and ordered the character.

**Character 191**. Middle to posterior cervical neural spines, distal expansion: (0) absent; (1) with a slight lateral distal border; (2) strongly expanded into a spine table.

This character originally coded for absence of a distal expansion and two different morphologies of such an expansion (Nesbitt, 2011). Nesbitt, Butler, Ezcurra, Barrett, et al. (2017) furthermore added a fourth character state for the moderately expanded dorsal borders in Aphanosauria. However, we found more variation in the shape of the spine tables in the middle to posterior cervicals of archosaurs, whereas we also considered it necessary to code if a spine table is generally absent or present. Thus, we divided this character into two

characters, one coding for the absence/presence of a spine table, and the other (new character 443) for the shape of this spine table in dorsal view. As the situation in Aphanosauria is not comparable to the spine table of other archosaurs, but can be distinguished, we kept this as a separate state in this unordered character.

**Character 291**. Ischium, medial contact with antimere: (0) restricted to the medial edge; (1) extensive contact, but dorsal margins are separated; (2) extensive contact up to the dorsal margin; (3) extensive contact, fused.

Originally, this character distinguished between three states, the three states retained here as state 0–2. However, taxa originally coded as 1 show some variation. Thus, in *Batrachotomus*, for example, the ischial shafts have a broad contact anteroventrally, but diverge postrodorsally, resulting in a heart-shaped outline of the articulated elements (SMNS 80280). In contrast, in many other taxa originally coded as 1, the ischial shafts contact over their entire medial surface, being only separated dorsally by a narrow groove marking the interischial suture. In contrast, in some poposaurids, for example, *Effigia* (Nesbitt, 2007), the ischia are fused without visible suture (see Schachner et al., 2020).

**Character 374**. Calcaneum, calcaneal tuber, distal end: (0) rounded and unexpanded; (1) markedly expanded dorsally.

In the original definition of the character, the derived state said that the distal end of the tuber is expanded both dorsally (proximally) and ventrally (distally). However, as some taxa, such as *Shuvosaurus* (Nesbitt, 2011) and *Schultzsuchus loricatus* have only a dorsal, but no ventral expansion, we decided to separate these two expansions into different characters (see new character 453).

**Character 439**. Anterior and middle cervical neural spines, shape in lateral view: (0) rectangular, sometimes with a slight expansion dorsally towards the spine table, vertical; (1), fan shaped, anteroposteriorly expanded dorsally; (2), rectangular, anteriorly inclined.

Originally, this character coded for an anterior overhang of the neural spine over the neural arch. However, the situation in distinct taxa showing such an overhang differs: whereas some, such as *Teleocrater* (Nesbitt, Butler, Ezcurra, Charig, & Barrett, 2017), *Xilousuchus* (Nesbitt et al., 2011) and *Schultzsuchus loricatus* have fan-shaped, dorsally anteriorly and posteriorly expanding neural spines, in other taxa, such as *Terrestrisuchus* (Crush, 1984) or *Ctenosauriscus* (Butler et al., 2011), the spine is rectangular, but slightly inclined anteriorly in its entirety. Thus, we separated these different character states.

## A.2. NEWLY ADDED CHARACTERS

**Character 440**. Ilium, dorsal margin of the iliac blade in postacetabular region, lateral view: (0) convex; (1) straight; (2) concave.

This character was proposed by Rezende et al. (2022; see discussion there), with state 2 representing an autapomorphy of *Prestosuchus*. However, although our analysis agrees that this state is a local autapomorphy of this taxon, state 2 is not restricted to *Prestosuchus*, but also found in *Riojasuchus* (von Baczko et al., 2020), the ilium originally referred to *Rauisuchus* (Lautenschlager & Rauhut, 2015), and an unidentified aetosaur ilium figured by Nesbitt (2011, figure 34E).

**Character 441**. Epipophysis in axis: (0) absent; (1) present.

In the original character list of Nesbitt et al. (2011), only the absence/presence of epipophyses in the anterior and posterior postaxial cervical vertebrae were coded for (characters 186 and 187, see above). However, not all taxa that have epipophyses in the postaxial cervicals also have epipophyses in the axis. Thus, within pseudosuchians, axial epipophyses are only found in *Revueltosaurus* (Parker et al., 2021), *Longosuchus* (TMM 31158-97), *Xilousuchus* (Nesbitt et al., 2011) and *Schultzsuchus*.

**Character 442**. Axis, posterior indentation in spinopostzygapophyseal lamina between postzygapophysis and posterior margin of neural spine: (0) present; (1) absent, lamina extends straight from postzygapophysis to the dorsal part of the neural spine.

In most archosaurs, the postzygapophyses of the axis project posteriorly beyond the posterior base of the neural spine, creating a concavity in the spinopostzygapophyseal laminae above the postzygapophyses in lateral view. In a few taxa, however, such as *Rauisuchus tiradentes* (Lautenschlager & Rauhut, 2015) and *Polonosuchus silesiacus* (Sulej, 2005), the spinopostzygapophyseal laminae extend straight posterodorsally from the postzygapophyses, so that a concavity is absent.

**Character 443**. Midcervical vertebrae, outline of distally expanded cervical neural spine in dorsal view: (0) rectangular or elliptical; (1) anteriorly expanded and narrowing posteriorly; (2) posteriorly expanded, narrowing anteriorly (heart shaped). Inapplicable in taxa that lack expanded cervical neural spines.

In his character 191, Nesbitt et al. (2011) coded for the presence of a spine table, and distinguished two distinct shapes of the distal end of the neural spine, one with the widest expansion at about the midsection of the spine, and one with the largest expansion anteriorly and tapering posteriorly, resulting in a triangular to heart-shaped spine in dorsal view. Thus, this character, which was treated as unordered, originally mixed two distinct aspects, one being the general absence/presence of a

feature, and the second its specific shape. Therefore, we decided to separate these two aspects into two distinct characters, as noted above. In addition, we found that several taxa, including *Stagonosuchus nyassicus* (GPIT RE 3831) and both species of *Postosuchus* (Peyer et al., 2008; Weinbaum, 2013) have a triangular or heart-shaped distal expansion, but with the greatest expansion at the posterior end and tapering anteriorly. Thus, we added a further character state.

**Character 444**. Midcervical vertebrae (C4–C6), ventral keel: (0) absent; (1) present.

A ventral keel is absent in the midcervical vertebrae of proterosuchids and the outgroup, *Mesosuchus*. However, most archosaurs have ventral keels in these vertebrae, usually developed as low, longitudinal ridges.

**Character 445**. Distal expansion of mid to posterior cervical neural spines: (0) more or less gradually expanding from the base to the tip; (1) abruptly expanding at the tip, spine T-shaped in anterior or posterior view. Inapplicable in taxa that lack expanded cervical neural spines.

In archosaurian taxa that have a thickened distal end of the cervical neural spines (a spine table, character 191), two different morphologies can be observed. In some taxa, such as *Euparkeria* (Ewer, 1965), *Fasolasuchus* (Bonaparte, 1981), or *Schultzsuchus*, the spine more or less gradually expands from its base towards the tip, whereas many other archosaurs show a spine of more or less equal width throughout most of its length, with an abrupt expansion at the tip, resulting in a T-shaped spine in anterior or posterior view (e.g., Gebauer, 2004; Gower & Schoch, 2009).

**Character 446**. Midcervical vertebrae, height of neural spines: (0) low, notably less than height of neural arch from centrum to top of postzygapophysis; (1) moderate, about as high as neural arch; (2) high, considerably higher than neural arch. ordered.

**Character 447**. Ratio of anteroposterior length to mediolateral width of midcervical neural spines (measured at approximately minimal anteroposterior length of spine, excluding distal expansions): (0) more than two; (1) less than two.

In most archosaurs, the cervical neural spines are anteroposteriorly elongate sheets of bone. However, in noncrocodylomorph loricatans, the spines are very short anteroposteriorly and thickened transversely (e.g., Gebauer, 2004; Gower & Schoch, 2009; Mastrantonio et al., in press; Weinbaum, 2013). The same morphology is also found in parasuchians (e.g., Long & Murry, 1995) and in the ornithosuchid *Riojasuchus* (von Baczko et al., 2020).

**Character 448**. Posterior cervical ribs, proximal shaft: (0) slender; (1) dorsoventrally expanded, forming a distinct anterior "keel."

Cervical ribs that are parallel to the vertebral column are a synapomorphy of archosauromorphs. In most taxa, the ribs are slender rods of bone that extend from the rib head posteriorly, although a short anterior process is also often present. In many noncrocodylomorph pseudosuchians, the proximal part of the cervical ribs is dorsoventrally expanded into a sheet of bone, forming a notable "keel" below the articular area. This morphology is also found in the parasuchian *Smilosuchus* (Nesbitt, 2011, figure 28J).

**Character 449**. Mid- to posterior dorsal vertebrae, prezygodiapophyseal lamina: (0) absent; (1) present.

Lateral lamination of the neural arch is present to varying degrees in the dorsal vertebrae of most archosauriform taxa (see Gower, 2001). However, a lamina connecting the prezygapophysis with the diapophysis above the parapophysis is absent in most pseudosuchians, with the notable exception of poposaurids (Nesbitt, 2005, 2007; Schachner et al., 2020). This lamina is also present in most dinosaur-line archosaurs.

**Character 450**. Anterior midcaudal vertebrae, median longitudinal groove in ventral surface of the centra (excluding anteriormost caudals): (0) absent; (1) present.

**Character 451**. Midcaudal neural spines, postspinal lamina defined by laterally, rather than posteriorly attaching spinopostzygapophyseal laminae: (0) absent; (1) present.

Most archosaurs have short spinopostzygapophyseal laminae in the caudal vertebrae that connect the lateral sides of the posterior margin of the neural spine with the postzygapophyses. In a few taxa, including *Batrachotomus* (Gower & Schoch, 2009), *Rauisuchus* (Lautenschlager & Rauhut, 2015), *Polonosuchus* (Sulej, 2005), *Postosuchus* (Weinbaum, 2013), and *Schultzsuchus*, these lamina are placed on the lateral side of the posterior part of the neural spine and extend lateroventrally, thus defining a low postspinal lamina on the posterior side of the spine.

**Character 452**. Ischial pit (depression in the iliac articulation of the ischium): (0) absent: (1) present.

Long and Murry (1995) and Weinbaum and Hungerbühler (2007) described a small, round depression in the wider posterior part of the iliac articulation of the ischium in *Poposaurus*, the ischial pit, which receives a corresponding process of the ilium. This pit was considered to be a diagnostic character of *Poposaurus* by these authors and also Nesbitt et al. (2011) and Schachner et al. (2020), but such a pit is also present in *Bromgroveia* (Nesbitt, 2005), *Shuvosaurus* (Long & Murry, 1995), and *Schultzsuchus*.

**Character 453**. Calcaneum, calcaneal tuber, distal end, ventral expansion: (0) absent; (1) present.

As noted above, the expansion of the calcaneal tuber was used as a character by Nesbitt (2011, character 374), but without making the distinction whether this structure is expanded only dorsally, or both dorsally and ventrally. As there is some variation in this character, and not all taxa that have a dorsal

expansion also show a ventral expansion of the tuber (e.g., *Schultzsuchus*, *Nundasuchus*, Nesbitt et al., 2014; *Teleocrater*, Nesbitt, Butler, Ezcurra, Charig, & Barrett, 2017), we separated these morphologies into different characters.

**Character 454**. Extensor groove in metatarsals (at least metatarsal III): (0) absent; (1) rounded to triangular and centrally placed, ±symmetrical; (2) elongate, obliquely laterodistally directed.

An extensor groove on the dorsal side of the distal end of the metatarsals (at least in metatarsal III) is absent in Prolacerta (Colbert, 1987; Gow, 1975) and a few archosauriforms. In most archosauriform taxa where such a groove is present, it is developed as a small, usually rounded or triangular depression on the dorsal surface of the distal end of the metatarsal. However, in a number of pseudosuchians, including *Schultzsuchus*, and silesaurids (e.g., Nesbitt, Langer, & Ezcurra, 2020), the extensor groove is developed as an elongated, oblique groove that extends from the dorsal surface of the distal metatarsal laterodistally.